Physics of Charged Particle Beams with Intense Self Field

Ronald C. Davidson

Plasma Physics Laboratory

Princeton University, Princeton, NJ 08543

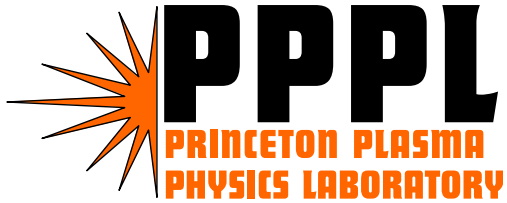

Workshop on Advanced Accelerator Concepts

Mandalay Beach, California

June 23 – 28, 2002

*Research supported by the U.S. Department of Energy.

Collaborators

- **Theory:**
  Hong Qin, Paul Channell, Igor Kaganovich, Wei-li Lee, Gennady Shvets, Edward Startsev, Sean Strasburg, Stephan Tzenov, and Tai-Sen Wang

- **Experiment:**
  Philip Efthimion, Eirk Gilson, Larry Grisham, and Richard Majeski.

Background:

- A fundamental understanding of nonlinear effects and collective processes on the propagation, acceleration, and compression of high-brightness, high-intensity charged particle beam is essential to the identification of optimum operating regimes in which emittance growth and beam losses are minimized.

- Collective processes and self-field effects become particularly important at the high beam intensities and luminosities envisioned in present and next-generation accelerators and transport systems for applications in:
  - High energy and nuclear physics.
  - Heavy Ion Fusion.

Physics of Intense Charged Particle Beams

- Develop and apply advanced theoretical techniques and simulation capabilities based on the nonlinear Vlasov-Maxwell equations to describe collective processes and nonlinear beam dynamics.

- Build on extensive theoretical literature and experimental data base developed in nonneutral plasma physics.

- Develop robust theoretical models capable of describing beam equilibrium, stability and transport properties over the entire range of normalized beam intensity s_b,

$$0 < s_b = \hat{\omega}_{pb}^2/2\gamma_b^2\omega_{\beta\perp}^2 < 1\,,$$

where $\omega_{\beta\perp}$ is the average transverse focusing frequency, and $\hat{\omega}_{pb}^2 = 4\pi\hat{n}_b e_b^2/\gamma_b m_b$ is the relativistic plasma frequency-squared.

What is Nonneutral Plasma?

- A nonneutral plasma is a many-body collection of charged particles in which there isn't overall charge neutrality.
- Such systems are characterized by intense self-electric fields (space-charge fields), and in high-current configurations by intense self-magnetic fields.
- Examples of nonneutral plasma systems include:
  - One-component nonneutral plasmas confined in a Malmberg-Penning trap or a Paul trap.
  - Intense charged particle beams and charge bunches in high energy accelerators, transport lines, and storage rings.
  - Coherent radiation sources (magnetrons, gyrotrons, free electron lasers).

Presentation Outline

- Nonlinear stability theorem
- Nonlinear perturbative simulations (BEST code)
- Collective two-stream interactions
- Instability driven by temperature anisotropy ($T_{\perp b} \gg T_{\|b}$).
- Hamiltonian averaging techniques
- Halo particle production by collective excitations
- Paul Trap Simulator Experiment

Presentation Outline

- Nonlinear stability theorem
- Nonlinear perturbative simulations (BEST code)
- Collective two-stream interactions
- Instability driven by temperature anisotropy ($T_{\perp b} \gg T_{\|b}$).
- Hamiltonian averaging techniques
- Halo particle production by collective excitations
- Paul Trap Simulator Experiment

Nonlinear Stability Theorem

Objective:

- Determine the class of beam distribution functions $f_b(\boldsymbol{x}, \boldsymbol{p}, t)$ that can propagate quiescently over large distances at high space-charge intensity.

Approach:

- Analysis makes use of global (spatially-averaged) conservation constraints satisfied by the nonlinear Vlasov-Maxwell equations to determine a sufficient condition for stability of an intense charged particle (or charge bunch) propagating in the z-direction with average axial velocity $V_b = const.$ along the axis of a perfectly-conducting cylindrical pipe with wall radius $r = (x^2 + y^2)^{1/2} = r_w$.

References:

- *Physics of Intense Charged Particle Beams in High Energy Accelerators* (World Scientific, 2001), R. C. Davidson and H. Qin, Chapter 4.

- "Kinetic Stability Theorem for High-Intensity Charged Particle Beams Based on the Nonlinear Vlasov-Maxwell Equations," R. C. Davidson, Physical Review Letters **81**, 991 (1998).

- "Three-Dimensional Kinetic Stability Theorem for High-Intensity Charged Particle Beams," R. C. Davidson, Physics of Plasmas **5**, 3459 (1998).

Theoretical Model and Assumptions

- Model makes use of fully nonlinear Vlasov-Maxwell equations for the self-consistent evolution of the distribution function $f_b(\boldsymbol{x}, \boldsymbol{p}, t)$ and self-generated electric and magnetic fields

$$\begin{aligned} \boldsymbol{E} &= -\nabla\phi - \frac{1}{c}\frac{\partial}{\partial t}\boldsymbol{A} \\ \boldsymbol{B} &= \nabla \times \boldsymbol{A} \end{aligned}$$

- Vlasov-Maxwell equations are Lorentz transformed to the beam frame ('primed' coordinates) where the (time-independent) confining potential of the applied focusing force is assumed to be of the form (smooth-focusing approximation)

$$\Psi'_{sf}(\boldsymbol{x}') = \frac{1}{2}\gamma_b\, m_b\, \omega_{\beta\perp}^2\, (x'^{\,2} + y'^{\,2}) + \frac{1}{2}\gamma_b\, m_b\, \omega_{\beta z}^2\, z'^{\,2},$$

  where $\omega_{\beta\perp}$ and $\omega_{\beta z}$ are constant focusing frequencies.

- Particle motions in the beam frame are assumed to be nonrelativistic.

Nonlinear Stability Theorem

In the beam frame, the nonlinear Vlasov-Maxwell equations possess (at least) two global conservation constraints corresponding to:

- Conservation of total energy

$$U(t') = \frac{1}{L'}\int d^3x' \left\{ \frac{|\boldsymbol{E}_T{}'|^2 + |\boldsymbol{B}_T{}'|^2}{8\pi} + \int d^3p' \left(\frac{\boldsymbol{p}'^2}{2\,m_b} + \Psi'_{sf} + \frac{1}{2} q_b\,\phi' \right) f_b \right\} = \text{const.}$$

- Conservation of generalized entropy

$$S(t') = \frac{1}{L'}\int d^3x'\, d^3p'\, G(f_b) = \text{const.}$$

Nonlinear Stability Theorem

- Consider general perturbations about a quasi-steady equilibrium distribution function $f_{eq}(\boldsymbol{x}', \boldsymbol{p}')$. For $f_{eq} = f_{eq}(H')$, using the global conservation constraints, it can be shown that

$$\frac{\partial}{\partial H'} f_{eq}(H') \leq 0$$

  is a sufficient condition for linear and nonlinear stability.

- Here,H' is the single-particle Hamiltonian defined by

$$H' = \frac{1}{2\, m_b} \boldsymbol{p}'^2 + \Psi'_{sf}(\boldsymbol{x}') + q_b\, \phi'(\boldsymbol{x}'),$$

  where $\phi'(\boldsymbol{x}')$ is the equilibrium space-charge potential.

Nonlinear Stability Theorem

- There is a wide range of choices of equilibrium distribution function $f_{eq}(H')$ that satisfy

$$\frac{\partial}{\partial H'} f_{eq}(H') \leq 0$$

and the equilibrium is therefore stable.

- One such distribution is the thermal equilibrium distribution

$$f_{eq} = g(H') \equiv \beta' \exp\left[-\frac{H'}{T_b'}\right],$$

where β' and T_b' are positive constants.

Nonlinear Stability Theorem

The three-dimensional stability theorem has a wide range of applicability to

- Perturbations about equilibria $f_{eq}(H')$ with arbitrary polarization and initial amplitude.
- *Continuous-beams* that are radially confined and infinite in axial extent ($\omega_{\beta\perp} \neq 0$, $\omega_{\beta z} = 0$).
- *Charge bunches* that are radially and axially confined ($\omega_{\beta\perp} \neq 0$, $\omega_{\beta z} \neq 0$).
- Beams with arbitrary space-charge intensity consistent with the requirement that the applied focusing potential $\Psi'_{sf}(\boldsymbol{x}')$ provides confinement of the beam particles.

Extension of Stability Theorem to General Confining Potential

- The stability theorem developed here has far wider applicability than to the case where $\Psi'_{sf}(\boldsymbol{x}')$ has the simple quadratic dependence on x', y', and z', provided the confining potential is time-stationary in the beam frame, i.e., $\partial\Psi'_{sf}/\partial t' = 0$.

- The main requirement on the $\boldsymbol{x}'$-dependence is that $\Psi'_{sf}(\boldsymbol{x}')$ correspond to a *confining* potential, i.e., that the focusing force $[\boldsymbol{F}_{foc}{}']_{sf} = -\nabla'\Psi'_{sf}$ is restoring.

PPPL PRINCETON PLASMA PHYSICS LABORATORY

Presentation Outline

- Nonlinear stability theorem
- ⇨ Nonlinear perturbative simulations (BEST code)
- Collective two-stream interactions
- Instability driven by temperature anisotropy ($T_{\perp b} \gg T_{\|b}$).
- Hamiltonian averaging techniques
- Halo particle production by collective excitations
- Paul Trap Simulator Experiment

Nonlinear Perturbative Particle Simulations

Objective:

⇨ For high intensity beam, it is increasingly important to develop an improved theoretical understanding of the influence of the intense self fields using a kinetic model based on the nonlinear Vlasov-Maxwell equations.

- ❍ Space-charge effects and collective instabilities.
- ❍ Collective mode structure, growth rates, and thresholds.
- ❍ Damping mechanisms and nonlinear wave-particle interactions.

Approach:

⇨ 3D multi-species nonlinear δf particle simulation code, called the Beam Equilibrium, Stability, and Transport (BEST) code, has been developed by Hong Qin. The BEST code is based on nonlinear Vlasov-Maxwell equations and provides a very effective tool for the investigating collective instabilities, self-field effects, and nonlinear beam dynamics.

- ❍ Significantly reduced simulation noise.
- ❍ Linear stability properties and nonlinear beam dynamics.

References (Illustrative):

- 3D Simulation Studies of the Two-Stream Instability in Intense Particle Beams Based on the Vlasov-Maxwell Equations, H. Qin, R. C. Davidson, W. W. Lee, and E. Startsev, Proceedings of the 2001 Particle Accelerator Conference, 696 (2001).

- 3D Multispecies Nonlinear Perturbative Particle Simulations of Collective Processes in Intense Particle Beams for Heavy Ion Fusion, H. Qin, R. C. Davidson, W. W. Lee, and R. Kolesnikov, Nuclear Instruments and Methods in Physics Research **A464**, 477 (2001).

- *Physics of Intense Charged Particle Beams in High Energy Accelerators* (World Scientific, 2001), R. C. Davidson and H. Qin, Chapter 8.

- 3D Multispecies Nonlinear Perturbative Particle Simulations of Collective Processes in Intense Particle Beams, H. Qin, R. C. Davidson, and W. W. Lee, Physical Review Special Topics – Accelerators and Beams **3**, 084401 (2000).

- 3D Nonlinear Perturbative Particle Simulations of Two-Stream Collective Processes in Intense Particle Beams, H. Qin, R. C. Davidson, and W. W. Lee, Physics Letter **A272**, 389 (2000).

Theoretical Model — Nonlinear Vlasov-Maxwell System

- Thin, continuous, high-intensity ion beam ($j = b$) propagates in the z-direction through background electron and ion components ($j = e, i$) described by distribution function $f_j(\boldsymbol{x}, \boldsymbol{p}, t)$.

- Transverse and axial particle velocities in a frame of reference moving with axial velocity $\beta_j c\hat{\boldsymbol{e}}_z$ are assumed to be *nonrelativistic*.

- Adopt a *smooth-focusing* model in which the focusing force is described by

$$\boldsymbol{F}_j^{foc} = -\gamma_j m_j \omega_{\beta j}^2 \boldsymbol{x}_\perp$$

- Self-electric and self-magnetic fields are expressed as

$$\begin{aligned} \boldsymbol{E}^s &= -\nabla\phi(\boldsymbol{x}, t) \\ \boldsymbol{B}^s &= \nabla \times \boldsymbol{A}_z(\boldsymbol{x}, t)\hat{\boldsymbol{e}}_z \end{aligned}$$

Theoretical Model — Nonlinear Vlasov-Maxwell System

⇨ Distribution functions and electromagnetic fields are described self-consistently by the nonlinear Vlasov-Maxwell equations in the six-dimensional phase space $(\boldsymbol{x}, \boldsymbol{p})$:

$$\left\{ \frac{\partial}{\partial t} + \boldsymbol{v} \cdot \frac{\partial}{\partial \boldsymbol{x}} - [\gamma_j m_j \omega_{\beta j}^2 \boldsymbol{x}_\perp + e_j (\nabla \phi - \frac{v_z}{c} \nabla_\perp A_z)] \cdot \frac{\partial}{\partial \boldsymbol{p}} \right\} f_j(\boldsymbol{x}, \boldsymbol{p}, t) = 0$$

and

$$\begin{aligned} \nabla^2 \phi &= -4\pi \sum_j e_j \int d^3 p f_j(\boldsymbol{x}, \boldsymbol{p}, t) \\ \nabla^2 A_z &= -\frac{4\pi}{c} \sum_j e_j \int d^3 p v_z f_j(\boldsymbol{x}, \boldsymbol{p}, t) \end{aligned}$$

Nonlinear δf Particle Simulation Method

- Divide the distribution function into two parts: $f_j = f_{j0} + \delta f_j$.
- f_{j0} is a known solution to the nonlinear Vlasov-Maxwell equations.
- Determine numerically the evolution of the perturbed distribution function $\delta f_j \equiv f_j - f_{j0}$.
- Advance the weight function defined by $w_j \equiv \delta f_j / f_j$, together with the particles' positions and momenta.
- Equations of motion for the particles are given by

$$\begin{aligned}
\frac{d\boldsymbol{x}_{\perp ji}}{dt} &= (\gamma_j m_j)^{-1} \boldsymbol{p}_{\perp ji}, \\
\frac{dz_{ji}}{dt} &= v_{zji} = \beta_j c + \gamma_j^{-3} m_j^{-1} (p_{zji} - \gamma_j m_j \beta_j c), \\
\frac{d\boldsymbol{p}_{ji}}{dt} &= -\gamma_j m_j \omega_{\beta j}^2 \boldsymbol{x}_{\perp ji} - e_j (\nabla\phi - \frac{v_{zji}}{c} \nabla_\perp A_z)
\end{aligned}$$

- Weight functions w_j are carried by the simulation particles, and the dynamical equations for w_j are derived from the definition of w_j and the Vlasov equation.

Nonlinear δf Particle Simulation Method

- Weight functions evolve according to

$$\begin{aligned} \frac{dw_{ji}}{dt} &= -(1-w_{ji})\frac{1}{f_{j0}}\frac{\partial f_{j0}}{\partial \boldsymbol{p}}\cdot\delta\left(\frac{d\boldsymbol{p}_{ji}}{dt}\right) \\ \delta\left(\frac{d\boldsymbol{p}_{ji}}{dt}\right) &\equiv -e_j(\nabla\delta\phi - \frac{v_{zji}}{c}\nabla_\perp\delta A_z) \end{aligned}$$

Here, $\delta\phi = \phi - \phi_0$, $\delta A_z = A_z - A_{z0}$, and $(\phi_0,\ A_{z0},\ f_{j0}\ )$ are the equilibrium solutions.

- The perturbed distribution function δf_j is given by the weighted Klimontovich representation

$$\delta f_j = \frac{N_j}{N_{sj}}\sum_{i=1}^{N_{sj}} w_{ji}\delta(\boldsymbol{x}-\boldsymbol{x}_{ji})\delta(\boldsymbol{p}-\boldsymbol{p}_{ji})$$

where N_j is the total number of actual j'th species particles, and N_{sj} is the total number of *simulation* particles for the j'th species.

Nonlinear δf Particle Simulation Method

⇨ Maxwell's equations are also expressed in terms of the perturbed quantities:

$$\nabla^2 \delta\phi = -4\pi \sum_j e_j \delta n_j$$

$$\nabla^2 \delta A_z = -\frac{4\pi}{c} \sum_j \delta j_{zj}$$

$$\delta n_j = \int d^3p \delta f_j(\boldsymbol{x}, \boldsymbol{p}, t) = \frac{N_j}{N_{sj}} \sum_{i=1}^{N_{sj}} w_{ji} S(\boldsymbol{x} - \boldsymbol{x}_{ji})$$

$$\delta j_{zj} = e_j \int d^3p v_z \delta f_j(\boldsymbol{x}, \boldsymbol{p}, t) = \frac{e_j N_j}{N_{sj}} \sum_{i=1}^{N_{sj}} v_{zji} w_{ji} S(\boldsymbol{x} - \boldsymbol{x}_{ji})$$

where $S(\boldsymbol{x} - \boldsymbol{x_{ji}})$ represents the method of distributing particles on the grids.

Advantages of the δf method

- Simulation noise is reduced significantly.
  - Statistical noise $\sim 1/\sqrt{N_s}$.
  - To achieve the same accuracy, number of simulation particles required by the δf method is only $(\delta f/f)^2$ times of that required by the conventional PIC method.
- No waste of computing resource on something already known — f_{j0}.
- Moreover, make use of the known (f_{j0}) to determine the unknown (δf_j).
- Study physics effects separately, as well as simultaneously.
- Easily switched between linear and nonlinear operation.

The BEST Code

Application of the 3D multispecies nonlinear δf simulation method is carried out using the Beam Equilibrium Stability and Transport (BEST) code at the Princeton Plasma Physics Laboratory.

- Adiabatic field pusher for light particles (electrons).
- Solves Maxwell's equations in cylindrical geometry.
- Written in Fortran 90/95 and extensively object-oriented.
- NetCDF data format for large-scale diagnostics and visualization.
- Achieved an average speed of 40μs/(particle$\times$step) on a DEC alpha personal workstation 500au computer.
- The code has been parallelized using OpenMP and MPI.
  - NERSC: IBM-SP2 Processors.
  - PPPL: Dec-α Processors.
- Achieved 2.0×10^{10} ion-steps + 4×10^{11} electron-steps for instability studies.

Nonlinear Properties of Equilibrium Proton Beam

- Single-species thermal equilibrium ion beam in a constant focusing field.
- Equilibrium properties depend on the radial coordinate $r = (x^2 + y^2)^{1/2}$.
- Cylindrical chamber with perfectly conducting wall located at $r = r_w$.
- Thermal equilibrium distribution function for the beam ion is given by

$$f_{b0}(r, \boldsymbol{p}) = \frac{\hat{n}_b}{\gamma_b^{5/2}(2\pi m_b T_b)^{3/2}} \exp\left[-\frac{H_\perp}{T_b}\right] \times \exp\left[-\frac{(p_z - \gamma_b m_b \beta_b c)^2}{2\gamma_b^3 m_b T_b}\right]$$

- As a benchmark test, system parameters are chosen to correspond to high-intensity proton beam in the Proton Storage Ring (PSR) experiment in the absence of background electrons, with normalized beam intensity $s_b = \hat{\omega}_{pb}^2/2\gamma_b^2\omega_{\beta b}^2 = 0.079$, and relativistic mass factor $\gamma_b = 1.85$.

Nonlinear Properties of Stable Proton Beam Propagation

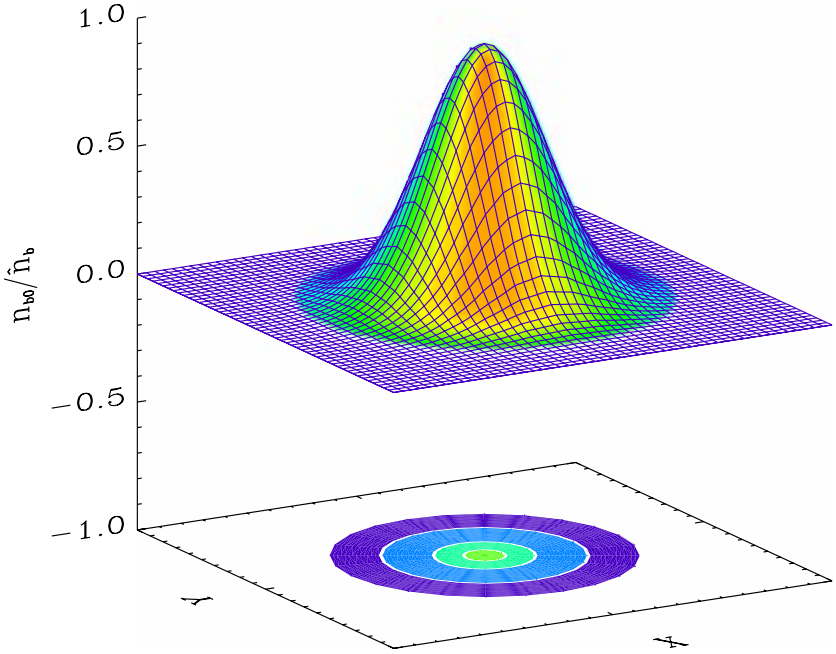

(a) Equilibrium Density

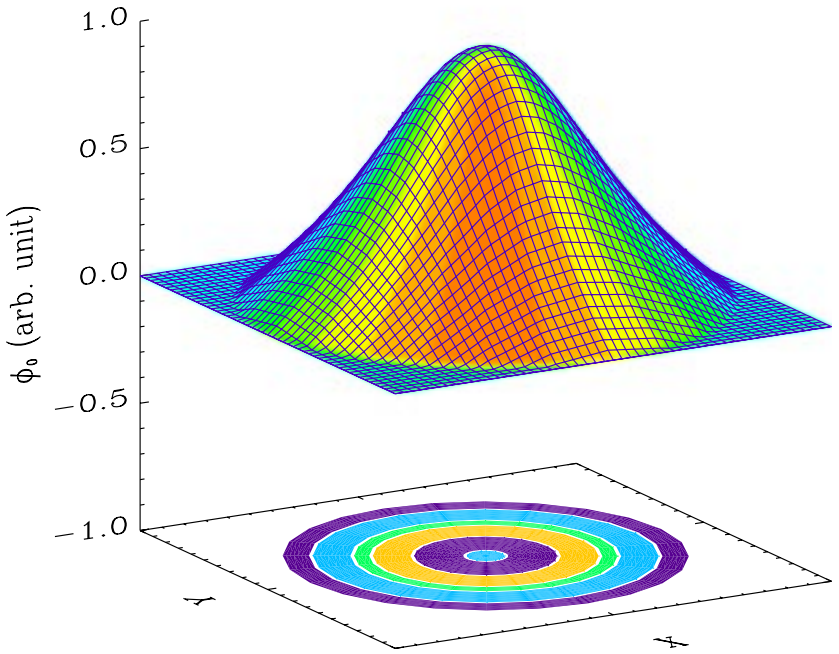

(b) Equilibrium Space-Charge Potential

- Equilibrium solutions (ϕ_0, A_{z0}, f_{j0}) solve the steady-state ($\partial/\partial t = 0$) Vlasov-Maxwell equations with $\partial/\partial z = 0$ and $\partial/\partial\theta = 0$.

Nonlinear Properties of Stable Proton Beam Propagation

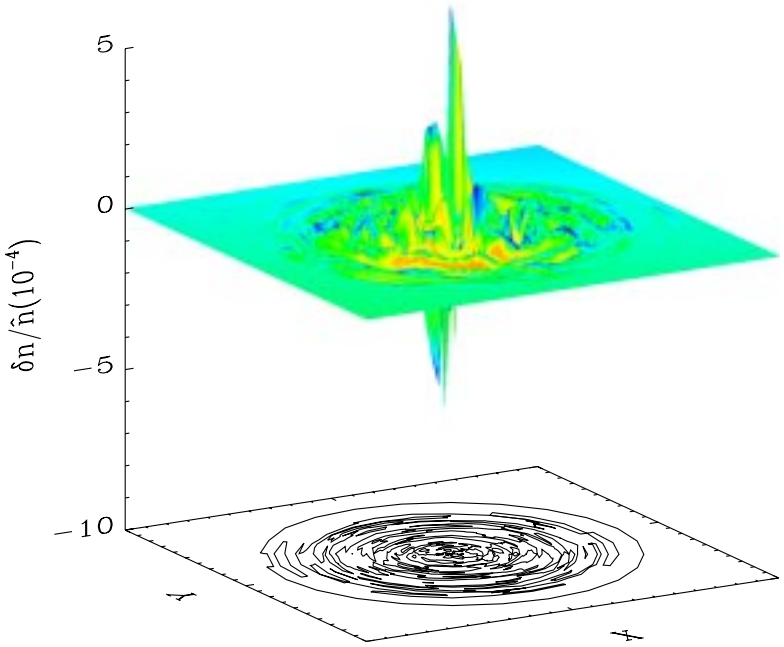

(a) Perturbed δn at $t = 0\tau_\beta$.

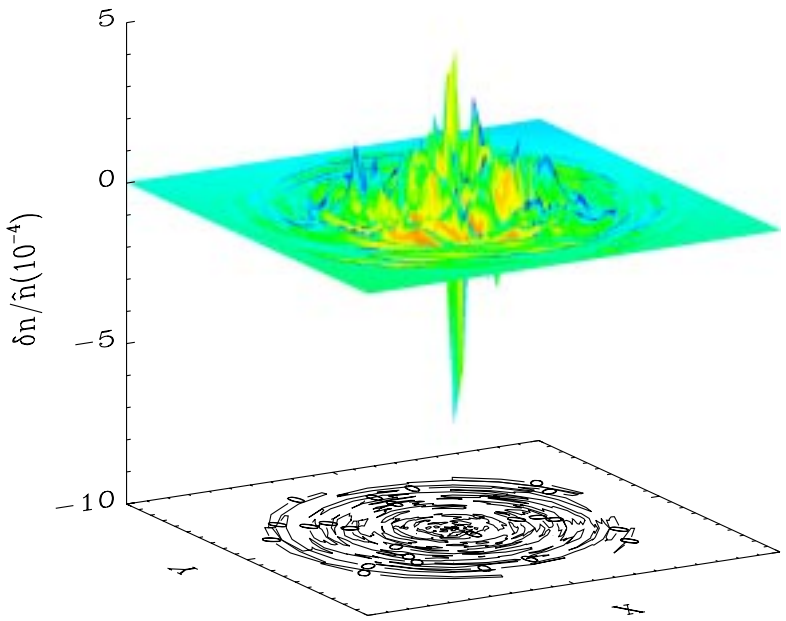

(b) Perturbed δn at $t = 3000\tau_\beta$.

- Random initial perturbation with normalized amplitudes of 10^{-3} are introduced into the system.
- The beam is propagated from $t = 0$ to $t = 3000\tau_\beta$, where $\tau_\beta \equiv \omega_{\beta b}^{-1}$.

Nonlinear Properties of Stable Proton Beam Propagation

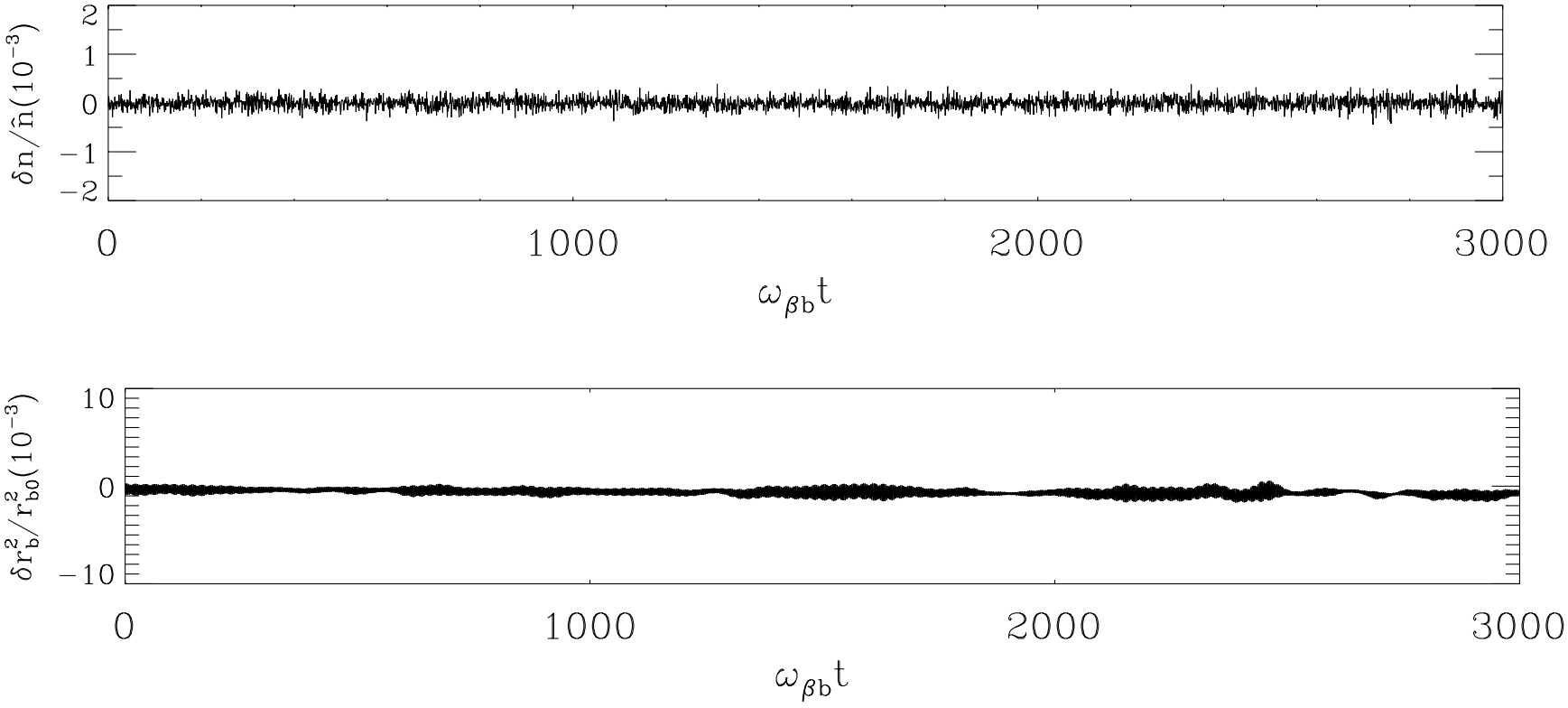

⇨ Simulation results show that the perturbations do not grow and the beam propagates quiescently, which agrees with the nonlinear stability theorem [Phys. Rev. Lett. **81**, 991 (1998)].

Body Modes by the BEST code

- Axisymmetric body modes with $l = 0$ and $k_z = 0$ for a moderate-intensity beam with $s_b \equiv \hat{\omega}_{pb}^2 / 2\gamma_b^2 \omega_{\beta b}^2 = 0.44$.
- First four body eigenmodes of the system at frequencies $\omega_1 = 1.53\ \omega_{\beta b}$, $\omega_2 = 2.98\ \omega_{\beta b}$, $\omega_3 = 4.50\ \omega_{\beta b}$, and $\omega_4 = 6.03\ \omega_{\beta b}$.
- Eigenfunction $\delta\phi_n(r)$ has n zeros when plotted as a function of r.

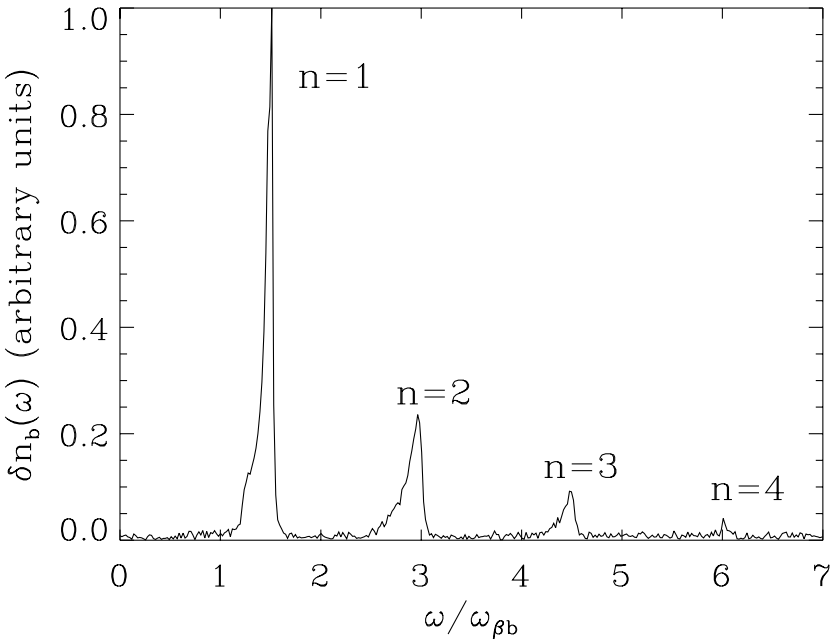

(a) Frequency spectrum

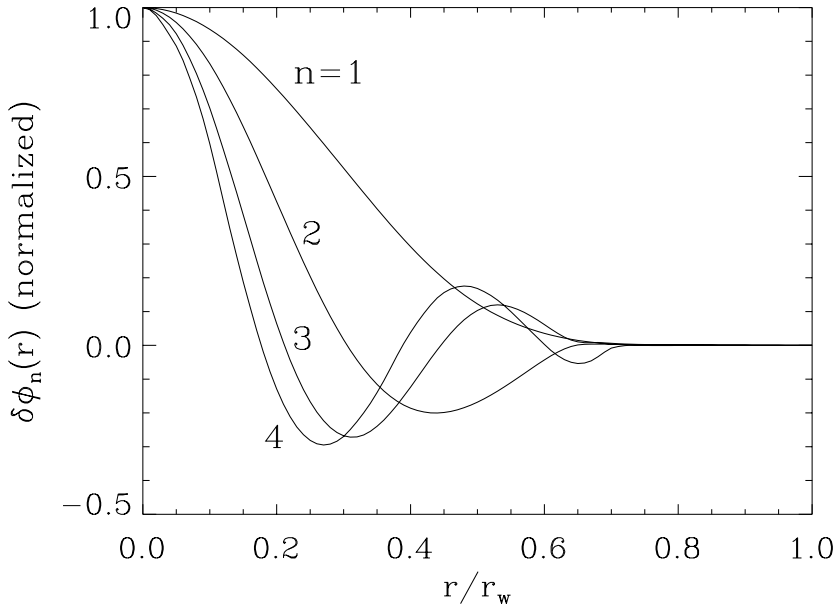

(b) Radial mode structure

Stable Surface Modes

- Linear surface modes for perturbations about a thermal equilibrium beam in the space-charge-dominated regime, with flat-top density profile.

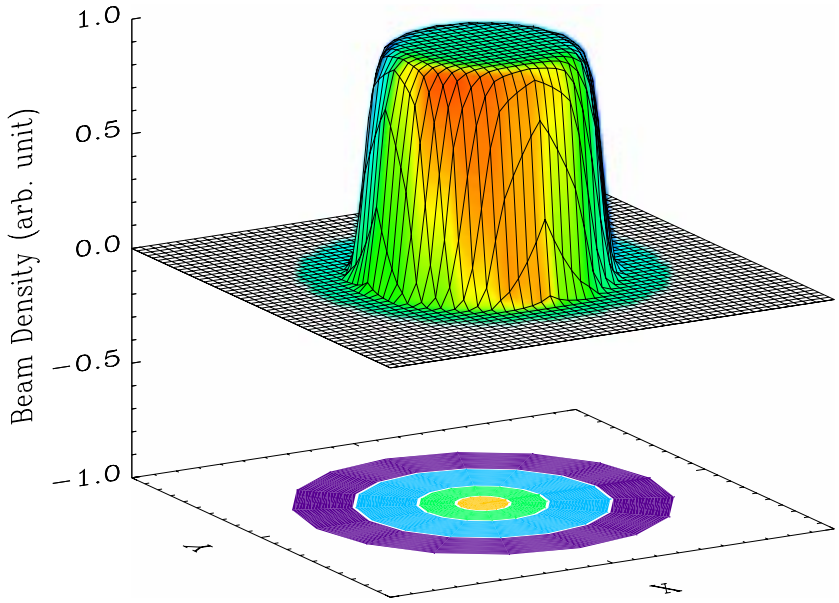

(a) Equilibrium Density

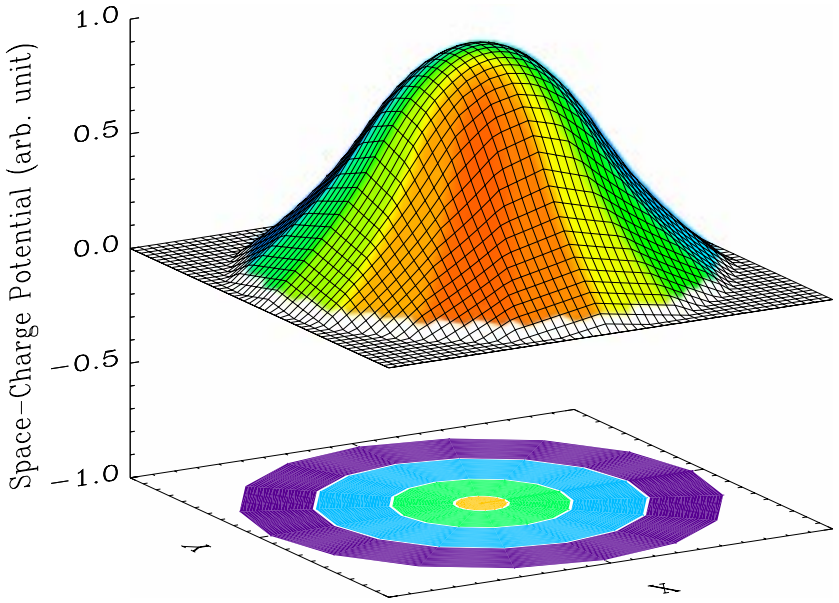

(b) Equilibrium Space-Charge Potential

Dipole Surface Modes

- The dipole surface modes can be destabilized by the electron-ion two-stream interaction when background electrons are present.
- The BEST code, operating in its linear stability mode, has recovered well-defined eigenmodes which agree with theoretical predications.

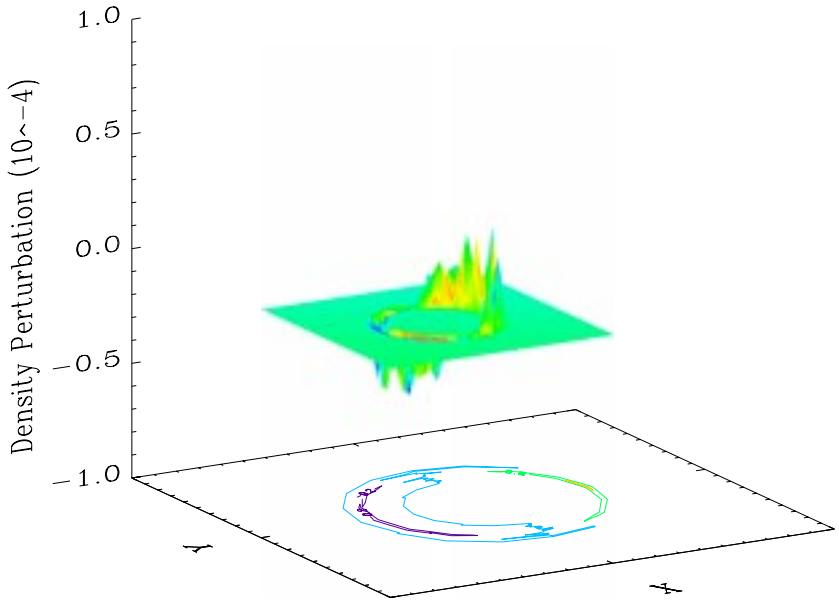

(a) Density Perturbation.

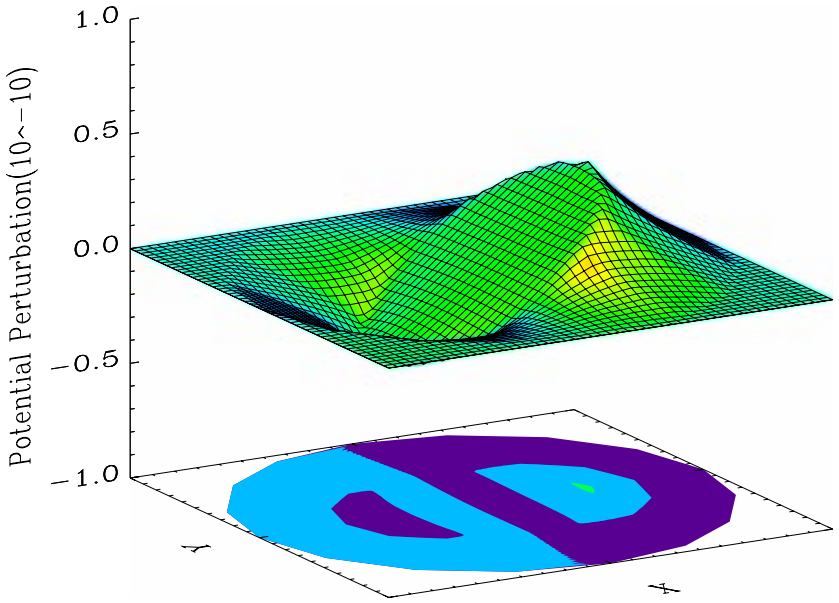

(b) Potential Perturbation.

Dipole Surface Modes (l=1)

- For azimuthal mode number $l = 1$, the dispersion relation is given by

$$\omega = k_z V_b \pm \frac{\hat{\omega}_{pb}}{\sqrt{2}\gamma_b}\sqrt{1 - \frac{r_b^2}{r_w^2}} \tag{1}$$

where r_b is the radius of the beam edge, and r_w is location of the conducting wall. Here, $\hat{\omega}_{pb}^2 = 4\pi\hat{n}_b e_b^2/\gamma_b m_b$ is the ion plasma frequency-squared, and $\hat{\omega}_{pb}/\sqrt{2}\gamma_b \backsimeq \omega_{\beta b}$ in the space-charge-dominated limit.

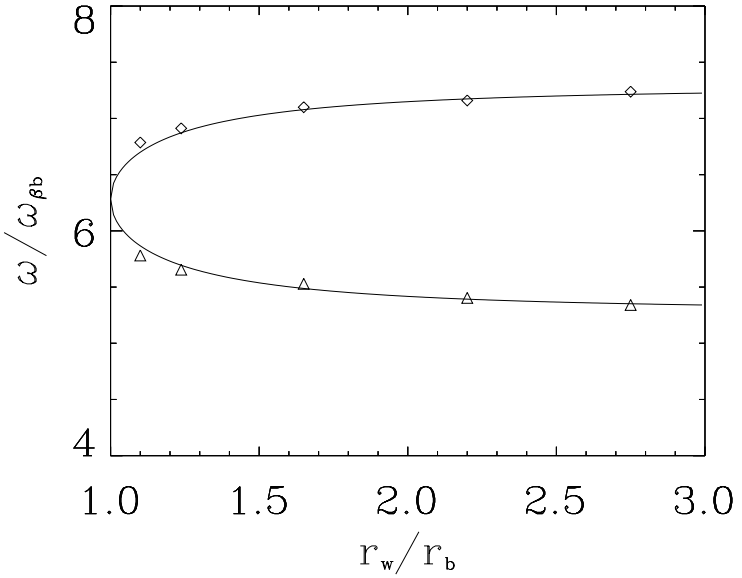

(a) $\omega/\omega_{\beta b}$ versus r_w/r_b

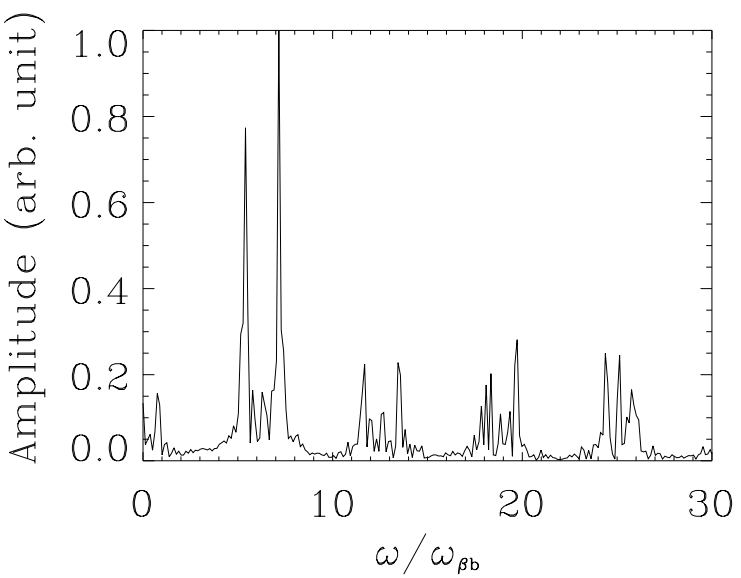

(b) Spectrum for $r_w/r_b = 2.2$

Presentation Outline

- Nonlinear stability theorem
- Nonlinear perturbative simulations (BEST code)
- ⇨ Collective two-stream interactions
- Instability driven by temperature anisotropy ($T_{\perp b} \gg T_{\|b}$).
- Hamiltonian averaging techniques
- Halo particle production by collective excitations
- Paul Trap Simulator Experiment

Two-Stream Instability for Intense Ion Beams

- In the absence of background electrons, an intense nonneutral ion beam supports collective oscillations (sideband oscillations) with phase velocity ω/k_z upshifted and downshifted relative to the average beam velocity $\beta_b c$.

- Introduction of an (unwanted) electron component (produced, for example, by secondary emission of electrons due to the interaction of halo ions with the chamber wall) provides the free energy to drive the classical two-stream instability.

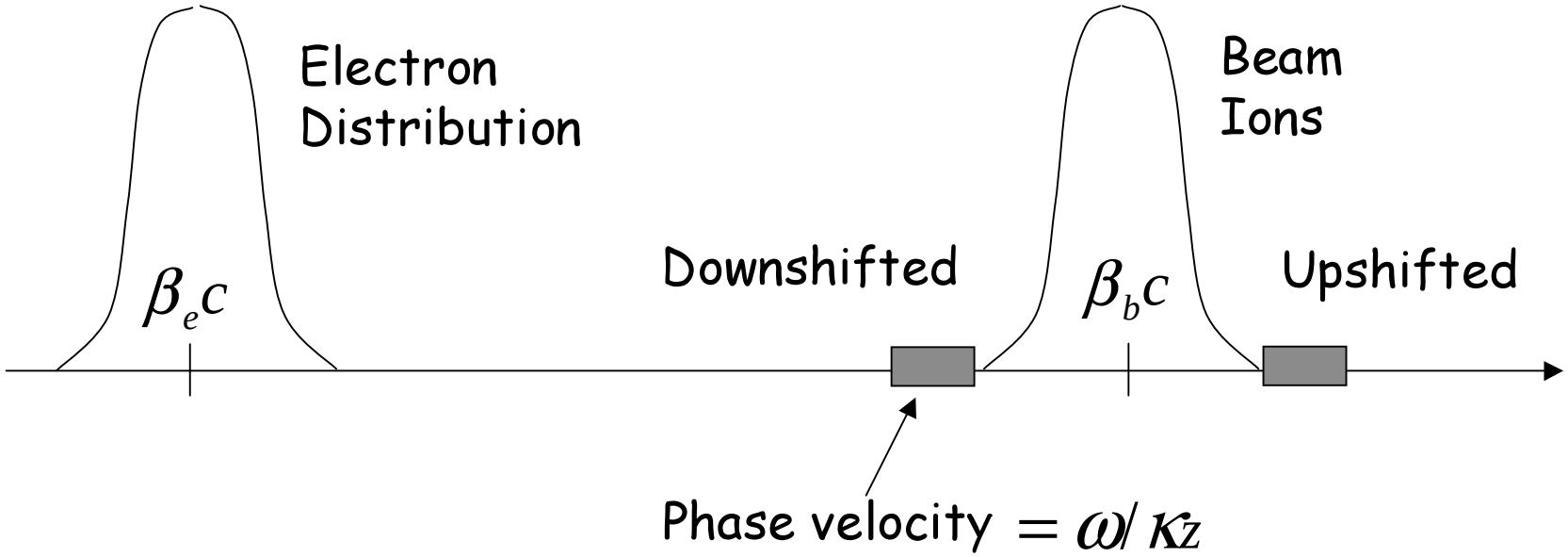

Two-Stream Instability for Intense Ion Beam

- Unlike the two-stream instability in a homogeneous neutral plasma, the two-stream instability for an intense, thin ion beam depends strongly on:
  - Transverse dynamics and geometry (r_b/r_w, $k_z r_b$).
  - Degree of charge neutralization ($f = \hat{n}_e/\hat{n}_b$).
  - Spread in transverse betatron frequencies.
  - Axial momentum spread.
- Strong experimental evidence for two-species instabilities:
  - Proton Storage Ring (PSR) at Los Alamos National Laboratory.
  - Beam-ion instability in electron machines.
  - Electron cloud instability in hadron machines.

$l = 1$ Dipole Mode in a Moderate-Intensity Proton Beam

- Generally, these is no analytical description of the eigenmodes in beams with nonuniform density profiles.
- However, numerical result shows that eigenmode is localized in the region where the density gradient is large.

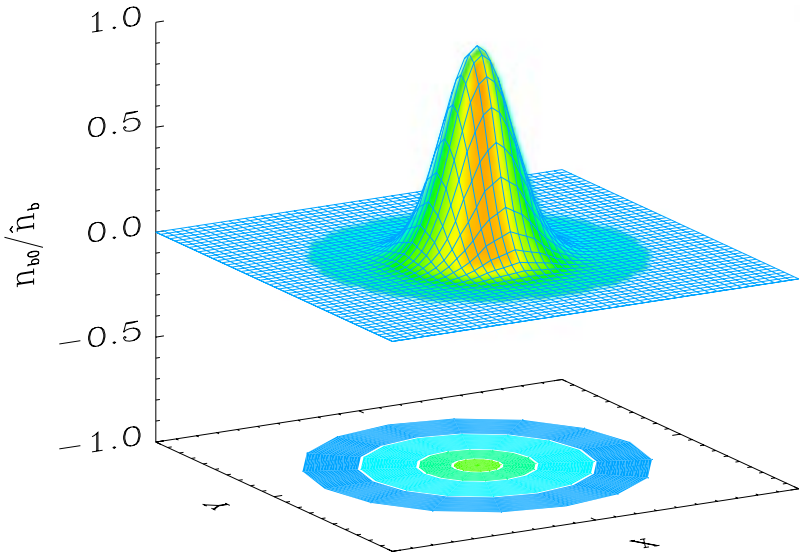

(a) Equilibrium Density Profile

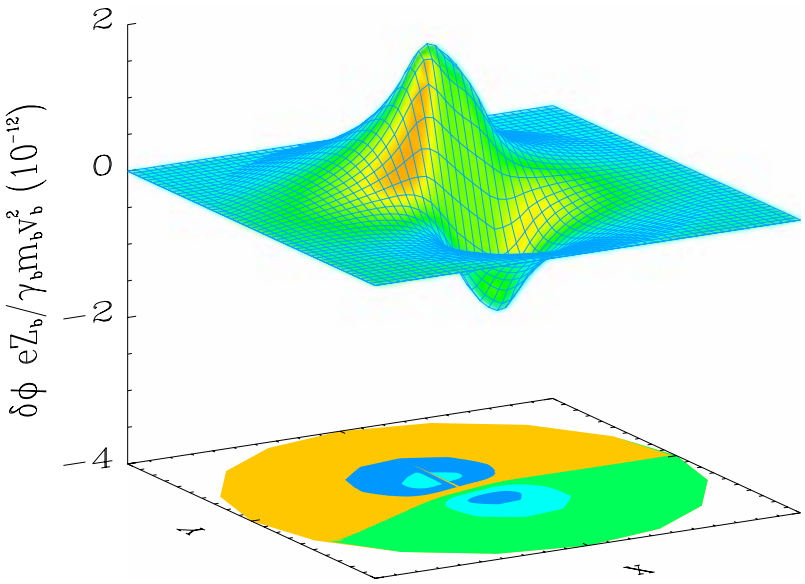

(b) Mode Structure

Electron-Proton Two-Stream Instability

- When a background electron component is introduced with $\beta_e = V_e/c \backsimeq 0$, the $l = 1$ dipole mode can be destabilized for a certain range of axial wavenumber and a certain range of electron temperature T_e.

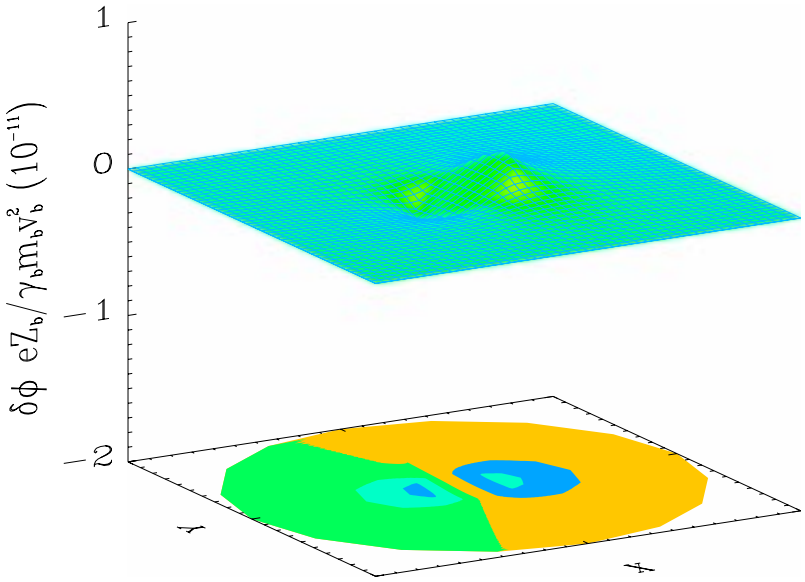

(a) $t = 0$

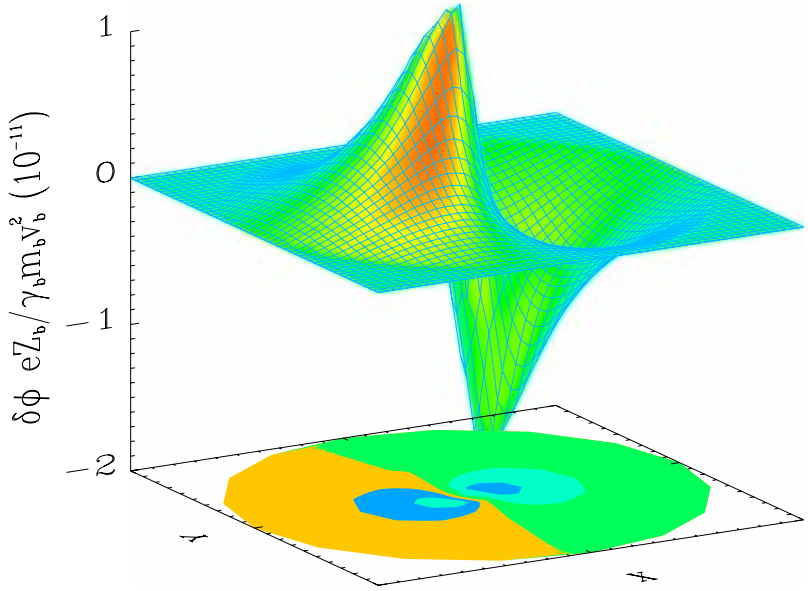

(b) $t = 200/\omega_{\beta_b}$

Growth Rate for Illustrative PSR Parameters

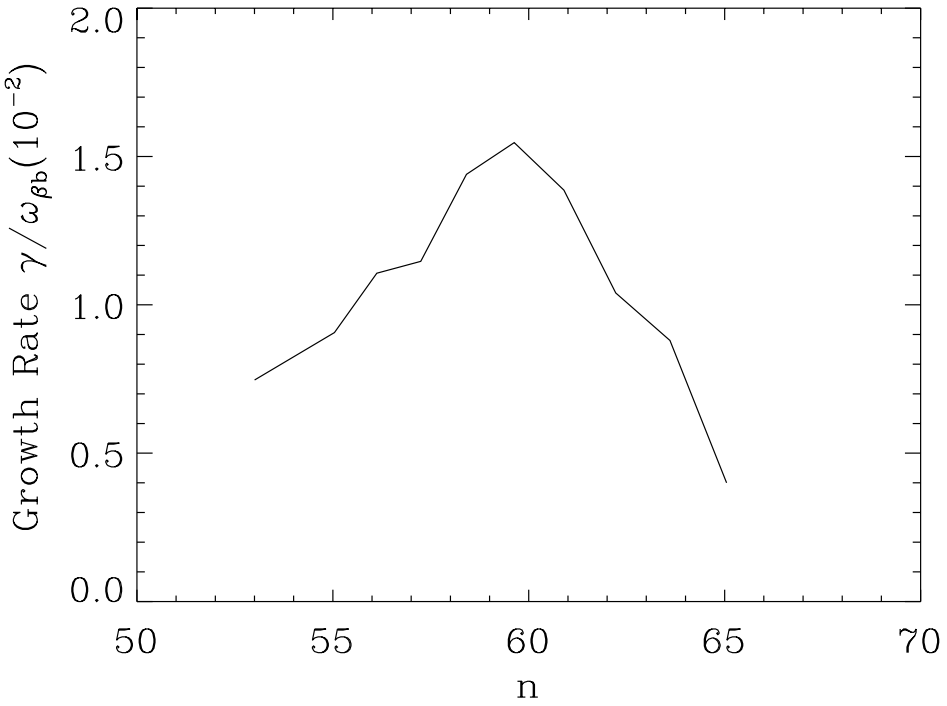

- Illustrative parameters in the Proton Storage Ring (PSR) experiment.
  - Space-charge-induced tune shift: $\delta\nu/\nu_0 \sim -0.020$, $\hat{\omega}_{pb}^2/2\gamma_b^2\omega_{\beta b}^2 = 0.079$.
  - Oscillation frequency (simulations): $f \sim 163$MHz. Mode number at maximum growth $n = 55 \sim 65$.
  - $\lambda_b = 9.13 \times 10^8 \mathrm{cm}^{-1}$, $\lambda_e = 9.25 \times 10^7 \mathrm{cm}^{-1}$, $T_{b\perp} = 4.41$keV, $T_{e\perp} = 0.73$keV, $\phi_0(r_w) - \phi_0(0) = -3.08 \times 10^3$Volts.

Growth Rate for Two-Stream Instability

- Maximum growth rate depends on the normalized beam density $\hat{n}_b/\hat{n}_{b0}$ and the initial axial momentum spread.

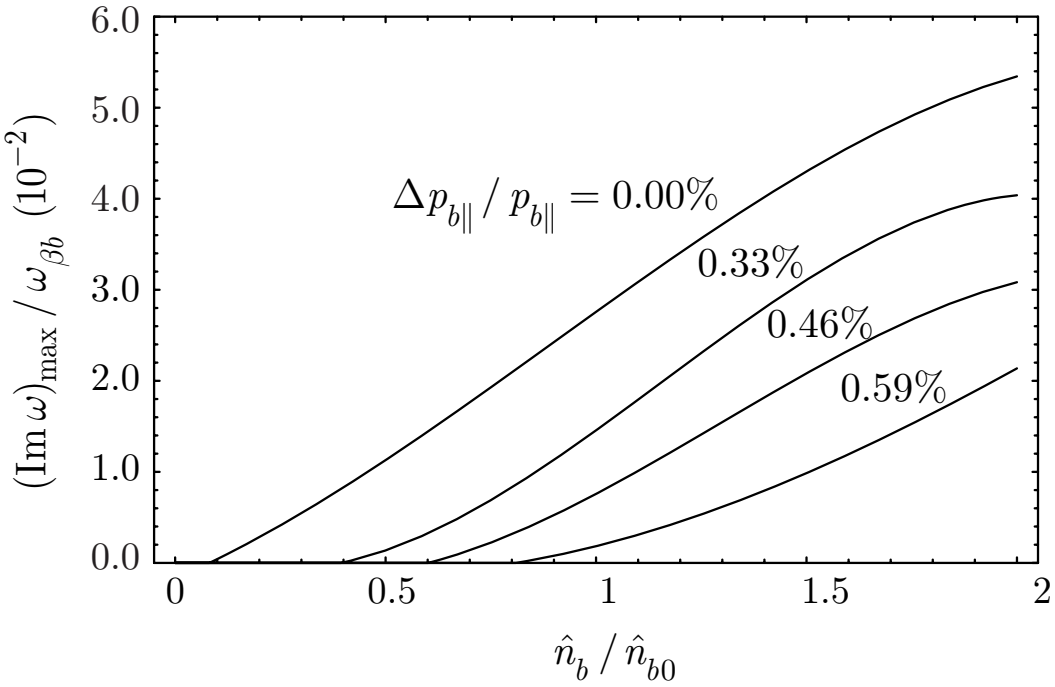

- $\hat{n}_{b0} = 9.41 \times 10^8 \mathrm{cm}^{-3}$, corresponding to an average current of 35 A in the Proton Storage Ring (PSR) experiment ($\hat{\omega}_{pb}^2/2\gamma_b^2\omega_{\beta b}^2 = 0.079$).

- A larger longitudinal momentum spread induces stronger Landau damping by parallel kinetic effects and therefore reduces the growth rate of the instability.

- Higher beam intensity provides more free energy to drive a stronger instability.

Instability Threshold

- Important damping mechanisms includes
  - Longitudinal Landau damping by the beam ions.
  - Stabilizing effects due to space-charge-induced tune spread.
- An instability threshold is observed in the simulations.

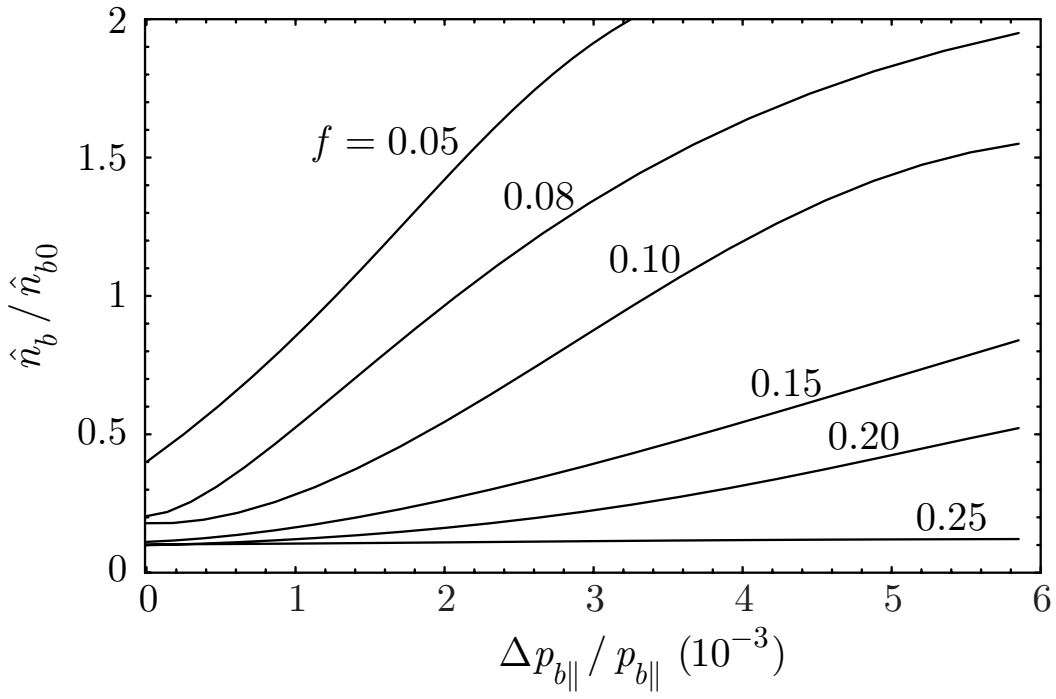

- Larger momentum spread and smaller fractional charge neutralization imply a higher density threshold for the instability to occur.

Long-Time Evolution of the e-p Instability

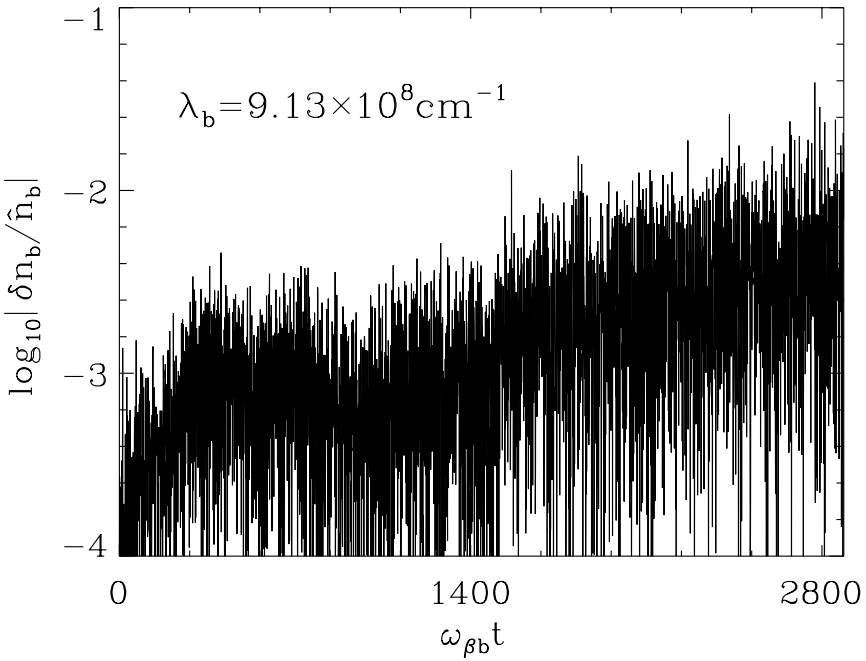

- Late-time nonlinear phase of e-p instability.
- Late-time nonlinear growth observed for system parameters above marginal stability.
- Simulations show two phases to the e-p instability.

Long-Time Evolution of the e-p Instability

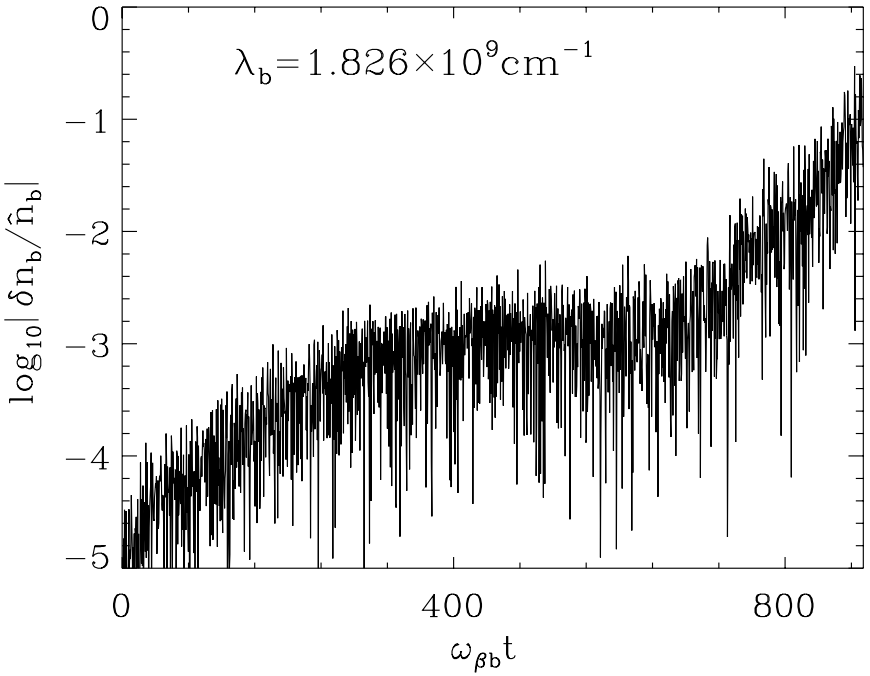

- Late-time nonlinear phase of e-p instability at twice the beam intensity.
- Nonlinear growth to larger amplitudes occurs on faster time scale.

Conclusions

- A 3D multispecies nonlinear perturbative particle simulation method has been developed to study two-stream instabilities in intense charged particle beams described self-consistently by the Vlasov-Maxwell equations.
- Introducing a background component of electrons, the two-stream instability is observed in the simulations. Several properties of this instability are investigated numerically, and are found to be in qualitative agreement with theoretical predictions.
- The self-consistent simulations show that the instability has a dipole mode structure, and the growth rate is an increasing function of proton density and fractional charge neutralization.
- The simulations show that an axial momentum spread and the space-charge induced tune spread provide effective stabilization mechanisms for the e-p instability.

PPPL PRINCETON PLASMA PHYSICS LABORATORY

Presentation Outline

- Nonlinear stability theorem
- Nonlinear perturbative simulations (BEST code)
- Collective two-stream interactions
- ⇨ Instability driven by temperature anisotropy ($T_{\perp b} \gg T_{\|b}$).
- Hamiltonian averaging techniques
- Halo particle production by collective excitations
- Paul Trap Simulator Experiment

Instability Driven by Large Temperature Anisotropy

PPPL PRINCETON PLASMA PHYSICS LABORATORY

Objective:

- Determine linear and nonlinear dynamics of intense beams with large temperature anisotropy ($T_{\perp b} >> T_{\|b}$).

Approach:

- Develop an analytical model based on linearized Vlasov-Maxwell equations to describe Harris-like instability in intense beams. Apply nonlinear δf BEST code to determine linear and nonlinear dynamics.

References:

- "Nonlinear δ F Simulation Studies of Intense Charged Particle Beams with Large Temperature Anisotropy," E. A. Startsev, R. C. Davidson and H. Qin, Phys. Plasmas **9**, in press (2002).
- "Delta-f Simulation Studies of the Stability Properties of Intense Charged Particle Beams with Temperature Anisotropy," E. A. Startsev, R. C. Davidson and H. Qin, Proceedings of the 2001 Particle Accelerator Conference, 3080 (2001).

Large Temperature Anisotropies ($T_{\perp b} >> T_{\|b}$) Develop Naturally in Accelerators

PPPL PRINCETON PLASMA PHYSICS LABORATORY

- For a beam of charged particles with charge q accelerated through a voltage V, the parallel temperature decreases according to

$$T_{\| f} = T^2{}_{\| i} / 2qV$$

- The transverse emittance and perpendicular temperature $T_{\perp b}$ can also increase relative to $T_{\|b}$ due to nonlinearities and mismatch.
- Free energy is available to drive a Harris-like instability which may lead to a deterioration of beam quality.

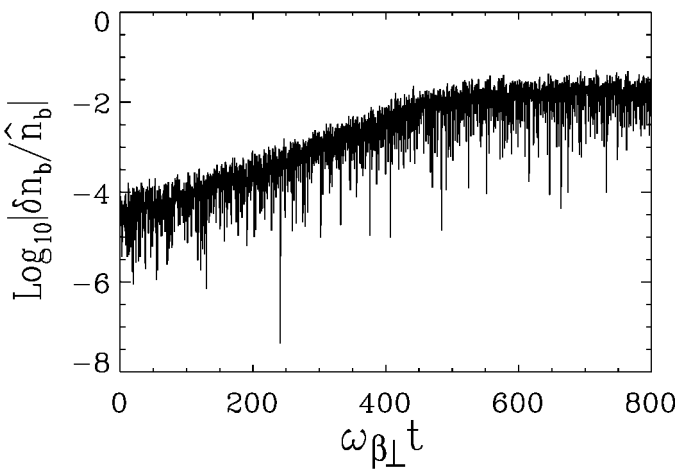

Assume axisymmetric perturbations.

Assume $T_{\|b} / T_{\perp b} = 0.04$ and $r_w / r_{beam} = 3.$

Low-noise properties of the BEST code allow one to follow the linear and nonlinear growth through saturation at the level $\left|\delta n_b^{\max} / \hat{n}_b\right| \cong 0.05.$

Onset and Saturation of the Instability

- Plot shows the net change in the longitudinal momentum distribution $\delta F_b(p_z)/\hat{F}_{0b}$, where

$$\delta F_b(p_z) = \int d^2 p_\perp d^3 x \delta f_b, \quad \hat{F}_{0b} = \hat{n}_b / (2\pi\gamma_b^3 m_b T_{\|b})^{1/2}.$$

- The formation of tails in the axial momentum distribution and the consequent saturation of the instability are attributed to resonant wave-particle interactions.

- The maximum growth rate $(\mathrm{Im}\omega)_{\max}/\omega_{\beta\perp} \cong 0.038$ occurs for $s_b = \hat{\omega}_{pb}^2 / 2\gamma_b^2 \omega_{\beta\perp}^2 \cong 0.8$, with no instability in the region $s_b \leq 0.5$.

- The instability is found to be absent if $T_{\|b} / T_{\perp b} > 0.07$.

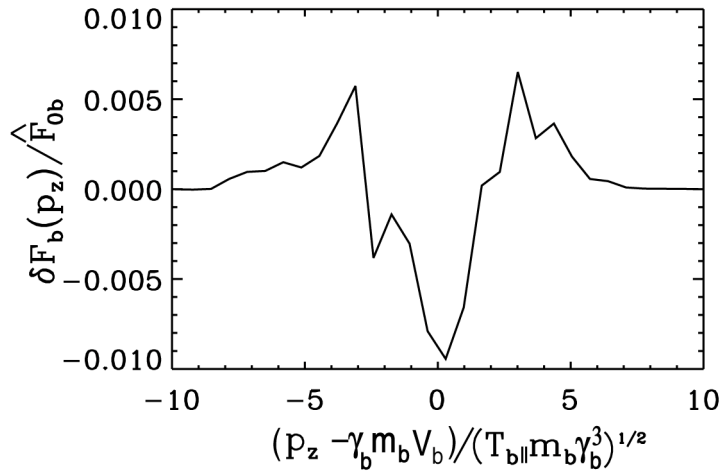

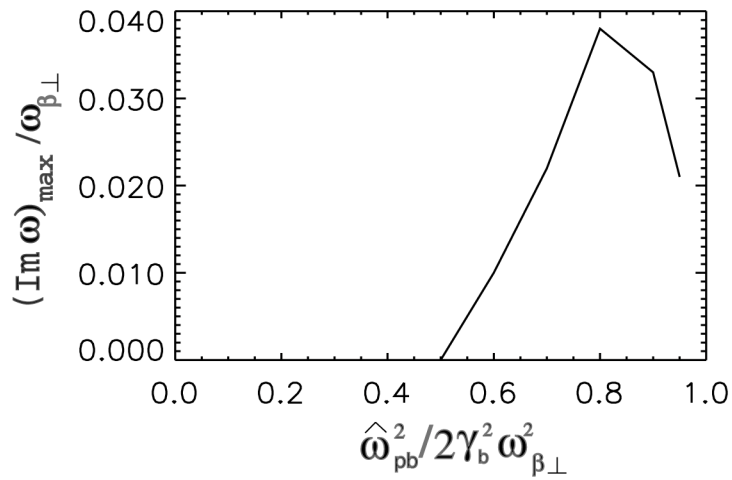

Instability Threshold

- The instability is stabilized by formation of a tail in the longitudinal momentum distribution and the consequent Landau damping of the wave excitations.
- The final width of the longitudinal velocity distribution can be estimated as $\Delta v_{||} \cong | v_{ph} - V_b |$, where $v_{ph} = \omega / k_z$.
- The growth rate $\gamma(T_{||b} = 0)$ for $T_{||b} = 0$ can be estimated as

$\gamma(T_{||b} = 0) \cong k_z (T_{||b}^{th} / \gamma_b^3 m_b)^{1/2}$, where $T_{||b}^{th}$ is the threshold temperature for stabilization.

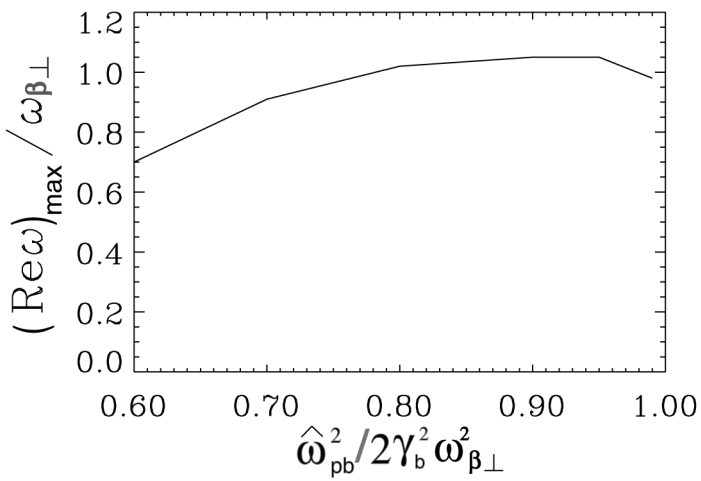

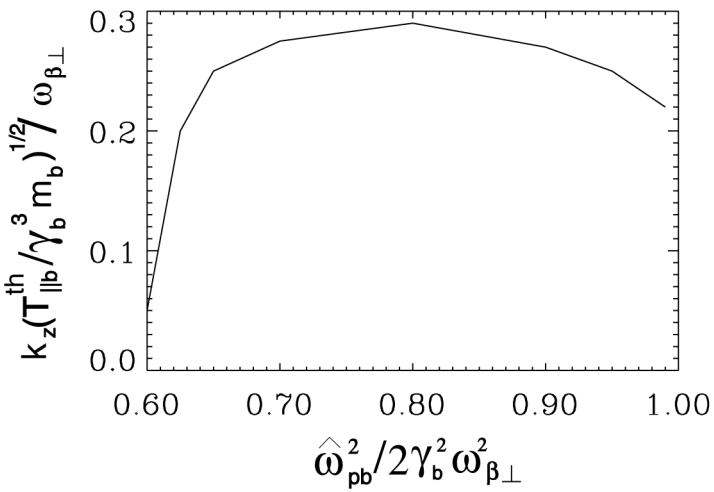

PPPL PRINCETON PLASMA PHYSICS LABORATORY

Presentation Outline

- Nonlinear stability theorem
- Nonlinear perturbative simulations (BEST code)
- Collective two-stream interactions
- Instability driven by temperature anisotropy ($T_{\perp b} \gg T_{\|b}$).
- ⇨ Hamiltonian averaging techniques
- Halo particle production by collective excitations
- Paul Trap Simulator Experiment

Hamiltonian Averaging Techniques

Objective

⇨ Develop a formalism based on the nonlinear Vlasov-Maxwell equations that can be used to investigate the equilibrium and stability properties of a general class of intense charged particle beam distributions propagating through periodic focusing field configurations.

Approach

⇨ Apply the third-order Hamiltonian averaging technique developed by Channell [Phys. Plasmas 6, 982 (1999)] to the specific example of intense beam propagation through a periodic focusing quadrupole field.

References

- "Approximate Periodically-Focused Solutions to the Nonlinear Vlasov-Maxwell Equations for Intense Beam Propagation Through an Alternating-Gradient Field", R. C. Davidson, H. Qin, and P. J. Channell, Physical Review Special Topics on Accelerators and Beams 2, 074401 (1999); 3, 029901 (2000).

- "Hamiltonian Formalism for Solving the Vlasov-Poisson Equations and its Application to Periodic Focusing Systems and the Coherent Beam-Beam Interactions", S. I. Tzenov and R. C. Davidson, Physical Review Special Topics on Accelerators and Beams 5, 021001 (2002).

- "Guiding-Center Vlasov-Maxwell Description of Intense Beam Propagation Through a Periodic Focusing Field", R. C. Davidson and H. Qin, Physical Review Special Topics on Accelerators and Beams 4, 104401 (2001).

Theoretical Model and Assumptions

- Consider a thin ($r_b \ll S$) intense nonneutral ion beam (ion charge $= +Z_b e$, rest mass $= m_b$) propagating in the z-direction through a periodic focusing quadrupole field with average axial momentum $\gamma_b m_b \beta_b c$, and axial periodicity length S.

- Here, r_b is the characteristic beam radius, $V_b = \beta_b c$ is the average axial velocity, and $(\gamma_b - 1)m_b c^2$ is the directed kinetic energy, where $\gamma_b = (1 - \beta_b^2)^{-1/2}$ is the relativistic mass factor.

- The particle motion in the beam frame is assumed to be nonrelativistic.

Theoretical Model and Assumptions

- Introduce the scaled 'time' variable

$$s = \beta_b ct$$

and the (dimensionless) transverse velocities

$$x' = \frac{dx}{ds} \quad \text{and} \quad y' = \frac{dy}{ds}$$

- The beam particles propagate in the z-direction through an alternating-gradient quadrupole field

$$\boldsymbol{B}_q^{foc}(\boldsymbol{x}) = B_q'(s)(y\hat{\boldsymbol{e}}_x + x\hat{\boldsymbol{e}}_y)$$

with lattice coupling coefficient defined by

$$\kappa_q(s) \equiv \frac{Z_b e B_q'(s)}{\gamma_b m_b \beta_b c^2}$$

Here, $B_q'(s) \equiv (\partial B_x^q/\partial y)_{(0,0)} = (\partial B_y^q/\partial x)_{(0,0)}$, and $x\hat{\boldsymbol{e}}_x + y\hat{\boldsymbol{e}}_y$ is the transverse displacement of a particle from the beam axis.

- Here,

$$\kappa_q(s+S) = \kappa_q(s)$$

where $S = const.$ is the axial periodicity length.

Theoretical Model and Assumptions

- Neglecting the axial velocity spread, and approximating $v_z \simeq \beta_b c$, the applied transverse focusing force on a beam particle is (inverse length units)

$$\boldsymbol{F}_{foc} = -\kappa_q(s)[x\hat{\boldsymbol{e}}_x - y\hat{\boldsymbol{e}}_y]$$

over the transverse dimensions of the beam ($r_b \ll S$).

- The (dimensionless) self-field potential experienced by a beam ion is

$$\psi(x,y,s) = \frac{Z_b e}{\gamma_b m_b \beta_b^2 c^2}[\phi(x,y,s) - \beta_b A_z(x,y,s)]$$

where $\phi(x,y,s)$ is the space-charge potential, and $A_z(x,y,s) \simeq \beta_b \phi(x,y,s)$ is the axial component of vector potential.

- The corresponding self-field force on a beam particle is (inverse length units)

$$\boldsymbol{F}_{self} = -\left[\frac{\partial \psi}{\partial x}\hat{\boldsymbol{e}}_x + \frac{\partial \psi}{\partial y}\hat{\boldsymbol{e}}_y\right]$$

Theoretical Model and Assumptions

- Transverse particle orbits $x(s)$ and $y(s)$ in the laboratory frame are determined from

$$\begin{aligned} \frac{d^2}{ds^2}x(s) + \kappa_q(s)x(s) &= -\frac{\partial}{\partial x}\psi(x,y,s) \\ \frac{d^2}{ds^2}y(s) - \kappa_q(s)y(s) &= -\frac{\partial}{\partial y}\psi(x,y,s) \end{aligned}$$

- The characteristic axial wavelength λ_q of transverse particle oscillations induced by a quadrupole field with amplitude $\hat{\kappa}_q$ is

$$\lambda_q \sim \frac{2\pi}{\sqrt{\hat{\kappa}_q}}$$

- The dimensionless small parameter ϵ assumed in the present analysis s is

$$\epsilon \sim \left(\frac{S}{\lambda_q}\right)^2 \sim \frac{\hat{\kappa}_q S^2}{(2\pi)^2} < 1,$$

which is proportional to the strength of the applied focusing field.

Theoretical Model and Assumptions

- The laboratory-frame Hamiltonian $\hat{H}(x, y, x', y', s)$ for single-particle motion in the transverse phase space (x, y, x', y') is

$$\begin{aligned} \hat{H}(x, y, x', y', s) &= \frac{1}{2}(x'^2 + y'^2) \\ &+ \frac{1}{2}\kappa_q(s)(x^2 - y^2) + \psi(x, y, s) \end{aligned}$$

- The Vlasov equation describing the nonlinear evolution of the distribution function $f_b(x, y, x', y', s)$ in laboratory-frame variables is given by

$$\begin{aligned} \left\{ \frac{\partial}{\partial s} + x'\frac{\partial}{\partial x} + y'\frac{\partial}{\partial y} \right. &- \left(\kappa_q(s)x + \frac{\partial \psi}{\partial x} \right) \frac{\partial}{\partial x'} \\ &\left. - \left(-\kappa_q(s)y + \frac{\partial \psi}{\partial y} \right) \frac{\partial}{\partial y'} \right\} f_b = 0, \end{aligned}$$

where $\psi(x, y, s) = e_b\phi^s(x, y, s)/\gamma_b^3 m_b \beta_b^2 c^2$ is the dimensionless self-field potential.

Theoretical Model and Assumptions

- The self-field potential $\psi(x, y, s)$ is determined self-consistently in terms of the distribution function $f_b(x, y, x', y', s)$ from

$$\left(\frac{\partial^2}{\partial x^2} + \frac{\partial^2}{\partial y^2}\right)\psi = -\frac{2\pi K_b}{N_b}\int dx'dy' f_b$$

- Here, $n_b(x, y, s) = \int dx'dy' f_b(x, y, x', y', s)$ is the number density of the beam ions, and the constants, K_b and N_b, are the self-field perveance and the number of beam ions per unit axial length, respectively, defined by

$$K_b = \frac{2N_b Z_b^2 e^2}{\gamma_b^3 m_b \beta_b^2 c^2} = const.$$

$$N_b = \int dxdydx'dy' f_b = const.$$

Canonical Transformation to Slow Variables

- Transform from laboratory-frame variables (x, y, x', y') to 'slow' variables (X, Y, X', Y') and new Hamiltonian $\mathcal{H}(X, Y, X', Y', s)$.
- Formalism employs a canonical transformation to transform away the rapidly oscillating terms in the laboratory-frame Hamiltonian.
- Formally express the laboratory-frame Hamiltonian as

$$\begin{aligned} H(x, y, x', y', s) &= \epsilon \hat{H}(x, y, x', y', s) \\ &= \epsilon \left[\frac{1}{2}(x'^2 + y'^2) + V(x, y, s) + \psi(x, y, s) \right] \end{aligned}$$

where ϵ is a small dimensionless parameter proportional to the focusing field strength.

- Here, $V(x, y, s)$ is the potential for the applied focusing field

$$V(x, y, s) = \frac{1}{2}\kappa_q(s)(x^2 - y^2)$$

where $\int_0^S ds \kappa_q(s) = 0$.

Canonical Transformation to Slow Variables

- Introduce a near-identity canonical transformation where the expanded generating function is defined by

$$S(x, y, X', Y', s) = xX' + yY' + \sum_{n=1}^{\infty} \epsilon^n S_n(x, y, X', Y', s)$$

- The transformed Hamiltonian $\mathcal{H}(X, Y, X', Y', s)$ in the slow variables is given by

$$\mathcal{H}(X, Y, X', Y', s) = H(x, y, x', y', s) + \frac{\partial}{\partial s} S(x, y, X', Y', s)$$

- Expressing $\mathcal{H} = \sum_{n=1}^{\infty} \epsilon^n \mathcal{H}_n$ gives

$$\begin{aligned} & \sum_{n=1}^{\infty} \epsilon^n \mathcal{H}_n(X, Y, X', Y', s) \\ = \; & \epsilon \left[\frac{1}{2}(x'^2 + y'^2) + V(x, y, s) + \psi(x, y, s) \right] \\ + \; & \sum_{n=1}^{\infty} \epsilon^n \frac{\partial}{\partial s} S_n(x, y, X', Y', s) \end{aligned}$$

Canonical Transformation to Slow Variables

- Solve for $S_n(x, y, X', Y', s)$, order by order, enforcing the requirement that the transformed Hamiltonian $\mathcal{H}(\tilde{X}, \tilde{Y}, \tilde{X}', \tilde{Y}', s)$ be slowly varying.

- This gives (correct to order ϵ^3) the slowly varying Hamiltonian

$$\begin{aligned}\mathcal{H}(\tilde{X}, \tilde{Y}, \tilde{X}', \tilde{Y}', s) &= \frac{1}{2}(\tilde{X}'^2 + \tilde{Y}'^2) \\ &+ \frac{1}{2}\kappa_f(\tilde{X}^2 + \tilde{Y}^2) + \psi(\tilde{X}, \tilde{Y}, s)\end{aligned}$$

- Here, κ_f is the *constant* focusing coefficient defined by

$$\kappa_f \equiv \kappa_{fq} = \frac{1}{S}\int_0^S ds[\alpha_q^2(s) - \langle\alpha_q\rangle^2]$$

$$\alpha_q(s) = \int_0^s ds\kappa_q(s)\ , \quad \langle\alpha_q\rangle = \frac{1}{S}\int_0^S ds\alpha_q(s)$$

Transformed Hamiltonian and Coordinate Transformation

- The coordinate transformation relating the laboratory-frame variables (x, y, x', y') to the slow variables $(\tilde{X}, \tilde{Y}, \tilde{X}', \tilde{Y}')$ is then given correct to order ϵ^3 by

$$\begin{aligned} x(\tilde{X}, \tilde{Y}, \tilde{X}', \tilde{Y}', s) &= [1 - \beta_q(s)]\tilde{X} + 2\left(\int_0^s ds\beta_q(s)\right)\tilde{X}' \\ y(\tilde{X}, \tilde{Y}, \tilde{X}', \tilde{Y}', s) &= [1 + \beta_q(s)]\tilde{Y} - 2\left(\int_0^s ds\beta_q(s)\right)\tilde{Y}' \end{aligned}$$

and

$$\begin{aligned} x'(\tilde{X}, \tilde{Y}, \tilde{X}', \tilde{Y}', s) &= [1 + \beta_q(s)]\tilde{X}' + \{-\alpha_q(s) + \langle\alpha_q\rangle\langle\alpha_q\rangle\beta_q(s) - \alpha_q(s)\beta_q(s) \\ &- \left(\int_0^s ds[\delta_q(s) - \langle\delta_q\rangle]\right)\}\tilde{X} + \left(\int_0^s ds\beta_q(s)\right)\frac{\partial}{\partial\tilde{X}}\left(\tilde{X}\frac{\partial\psi}{\partial\tilde{X}} - \tilde{Y}\frac{\partial\psi}{\partial\tilde{Y}}\right) \\ y'(\tilde{X}, \tilde{Y}, \tilde{X}', \tilde{Y}', s) &= [1 - \beta_q(s)]\tilde{Y}' + \{\alpha_q(s) - \langle\alpha_q\rangle + \langle\alpha_q\rangle\beta_q(s) - \alpha_q(s)\beta_q(s) \\ &- \left(\int_0^s ds[\delta_q(s) - \langle\delta_q\rangle]\right)\}\tilde{Y} - \left(\int_0^s ds\beta_q(s)\right)\frac{\partial}{\partial\tilde{Y}}\left(\tilde{Y}\frac{\partial\psi}{\partial\tilde{Y}} - \tilde{X}\frac{\partial\psi}{\partial\tilde{X}}\right) \end{aligned}$$

Nonlinear Vlasov-Maxwell Equations in the Transformed Variables

- For the transformed Hamiltonian, the single-particle equations of motion are given by

$$\frac{d}{ds}\tilde{\boldsymbol{X}} = \frac{\partial \mathcal{H}}{\partial \tilde{\boldsymbol{X}}'} = \tilde{X}'\hat{\boldsymbol{e}}_x + \tilde{Y}'\hat{\boldsymbol{e}}_y$$

$$\frac{d}{ds}\tilde{\boldsymbol{X}}' = -\frac{\partial \mathcal{H}}{\partial \tilde{\boldsymbol{X}}} = -\kappa_f(\tilde{X}\hat{\boldsymbol{e}}_x + \tilde{Y}\hat{\boldsymbol{e}}_y) - \frac{\partial}{\partial \tilde{\boldsymbol{X}}}\psi(\tilde{X}, \tilde{Y}, s)$$

- The nonlinear Vlasov equation for the distribution function $F_b(\tilde{X}, \tilde{Y}, \tilde{X}', \tilde{Y}', s)$ in the transformed variables is then given by

$$\left\{\frac{\partial}{\partial s} + \tilde{X}'\frac{\partial}{\partial \tilde{Y}} + \tilde{Y}'\frac{\partial}{\partial \tilde{Y}} - \left(\kappa_f \tilde{X} + \frac{\partial}{\partial \tilde{X}}\psi\right)\frac{\partial}{\partial \tilde{X}'}\right.$$

$$\left. - \left(\kappa_f \tilde{Y} + \frac{\partial}{\partial \tilde{Y}}\psi\right)\frac{\partial}{\partial \tilde{Y}'}\right\} F_b(\tilde{X}, \tilde{Y}, \tilde{X}', \tilde{Y}', s) = 0$$

Nonlinear Vlasov-Maxwell Equations in the Transformed Variables

- The characteristics of the Vlasov equation correspond to the single-particle equations of motion in the applied-field plus self-field configuration.

- The slowly-varying self-field potential $\psi(\tilde{X},\tilde{Y},s)$ is determined self-consistently in terms of the distribution function $F_b(\tilde{X},\tilde{Y},\tilde{X}',\tilde{Y}',s)$ from

$$\left(\frac{\partial^2}{\partial\tilde{X}^2} + \frac{\partial^2}{\partial\tilde{Y}^2}\right)\psi(\tilde{X},\tilde{Y},s) = -\frac{2\pi K_b}{N_b}\int d\tilde{X}'d\tilde{Y}'F_b(\tilde{X},\tilde{Y},\tilde{X}',\tilde{Y}',s)$$

- Because the coordinate transformation is canonical, the laboratory-frame distribution function $f_b(x,y,x',y',s)$ is related to the transformed distribution function $F_b(\tilde{X},\tilde{Y},\tilde{X}',\tilde{Y}',s)$ by

$$f_b(x,y,x',y',s)dxdydx'dy' = F_b(\tilde{X},\tilde{Y},\tilde{X}',\tilde{Y}',s)d\tilde{X}d\tilde{Y}d\tilde{X}'d\tilde{Y}'$$

Nonlinear Vlasov-Maxwell Equations in the Transformed Variables

- The Jacobian of the transformation is equal to unity

$$\frac{\partial(x, y, x', y')}{\partial(\tilde{X}, \tilde{Y}, \tilde{X}', \tilde{Y}')} = 1$$

  which can also be verified correct to order ϵ^3 by *direct calculation.*

- Nonlinear Vlasov-Maxwell equations for $F_b(\tilde{X}, \tilde{Y}, \tilde{X}', \tilde{Y}', s)$ and $\psi(\tilde{X}, \tilde{Y}, s)$ in the slow variables $(\tilde{X}, \tilde{Y}, \tilde{X}', \tilde{Y}')$ can be used to investigate detailed equilibrium and stability properties over a wide range of system parameters, including beam intensity $[K_b]$ and choice of periodic lattice function $[\kappa_q(s)]$.

- Because the focusing coefficient is constant ($\kappa_f = const.$) in the transformed variables, analysis of the nonlinear Vlasov-Maxwell equations for $F_b(\tilde{X}, \tilde{Y}, \tilde{X}', \tilde{Y}', s)$ and $\psi(\tilde{X}, \tilde{Y}, s)$ is far more amenable to direct calculation than the nonlinear Vlasov-Maxwell equations for $f_b(x, y, x', y', s)$ and $\psi(x, y, s)$ in laboratory-frame variables.

- Because $\kappa_f = const.$ in the transformed variables, a wide body of kinetic equilibrium and stability literature derived in the constant-focusing case can be applied virtually intact.

Nonlinear Vlasov-Maxwell Equations in the Transformed Variables

- Because the focusing force, $\boldsymbol{F}_{foc} = -\kappa_f(\tilde{X}\hat{e}_x + \tilde{Y}\hat{\boldsymbol{e}}_y)$, is isotropic in the transverse plane, the nonlinear Vlasov-Maxwell equations for $F_b(\tilde{X}, \tilde{Y}, \tilde{X}', \tilde{Y}', s)$ and $\psi(\tilde{X}, \tilde{Y}, s)$ support a broad class of equilibrium solutions $(\partial/\partial s = 0)$ which are axisymmetric $(\partial/\partial\Theta = 0)$ in the transformed variables.

- The corresponding solutions for $f_b(x, y, x', y', s)$ and $\psi(x, y, s)$ in laboratory-frame variables, however, are periodically focused with axial periodicity length $S = const.$

- While the transformed variables $(\tilde{X}, \tilde{Y})$ are 'space-like' and $(\tilde{X}', \tilde{Y}')$ are 'velocity-like', it is important to keep in mind that the dependence of (x, y, x', y') on $(\tilde{X}, \tilde{Y}, \tilde{X}', \tilde{Y})$ is inexorably mixed by the coordinate transformation derived earlier.

PPPL PRINCETON PLASMA PHYSICS LABORATORY

Conclusions

- The present formalism represents a powerful framework for describing periodically-focused beam propagation through an alternating-gradient quadrupole focusing field, $\kappa_q(s+S) = \kappa_q(s)$, at arbitrary beam intensity.

- Circular cross-section beam equilibria in the transformed variables $(\tilde{X}, \tilde{Y}, \tilde{X}', \tilde{Y}')$, *back-transform* to periodically-focused pulsating beam distribution functions with elliptical cross-section in the laboratory-frame variables (x, y, x', y').

- Because $\kappa_f = const.$ in the transformed variables, a large body of constant-focusing equilibrium and stability results can be applied virtually intact.

Conclusions

- One key result is the kinetic stability theorem, which demonstrates that $(\partial/\partial\mathcal{H}^0)F_b^0(\mathcal{H}_0) \leq 0$ is a sufficient condition for stability (linear and nonlinear).

- Within the context of the present analysis, there are numerous beam equilibria $F_b^0(\mathcal{H}^0)$ in the transformed variables $(\tilde{X}, \tilde{Y}, \tilde{X}', \tilde{Y})$, with corresponding (periodically-focused) beam distributions in laboratory-frame variables (x, y, x', y').

- No longer is the Kapchinskij-Vladimirskij (KV) distribution the *only known periodically-focused* solution to the nonlinear Vlasov-Maxwell equations.

Presentation Outline

- Nonlinear stability theorem
- Nonlinear perturbative simulations (BEST code)
- Collective two-stream interactions
- Instability driven by temperature anisotropy ($T_{\perp b} \gg T_{\|b}$).
- Hamiltonian averaging techniques
- ⇨ Halo particle production by collective excitations
- Paul Trap Simulator Experiment

Halo Particle Production by Collective Excitations in Intense Beams

Background

- Frequently explored mechanisms for production of halo particles in intense beams include beam mismatch, envelope instabilities, and nonuniform charge density, using test-particle and particle-core models as appropriate.

Recent Developement

- Collective wave excitations, even in a matched beam, provide an additional mechanism for ejecting halo particles from the beam core.

References

- "Production of Halo Particles by Excitation of Collective Modes in High-Intensity Charged Particle Beams," S. Strasburg and R. C. Davidson, Physical Review **E61**, 5753 (2000).

- "Warm-Fluid Collective Mode Excitations in Intense Charged Particle Beams – Test Particle Simulations", S. Strasburg and R. C. Davidson, Nucl. Instr. and Meth. in Phys. Res. **A464**, 524 (2001).

Theoretical Model

- Assume collective oscillations about an intense axisymmetric beam ($\partial/\partial\theta = 0$) in the smooth-focusing approximation with applied focusing force

$$\boldsymbol{F}_{foc} = -\gamma_b m_b \omega_{\beta b}^2 (x\hat{\boldsymbol{e}}_x + y\hat{\boldsymbol{e}}_y).$$

- Assume matched-beam equilibrium (constant rms radius), and follow the test-particle motion, including the combined effects of the applied focusing and equilibrium space-charge forces, and the self-consistent collective oscillations.

- Electrostatic potential is expressed as

$$\phi(r,t) = \phi(r) + \delta\phi(r,t)$$

where the oscillating potential $\delta\phi$ is calculated self-consistently using the warm-fluid model for perturbations about a step-function waterbag density profile (Lund and Davidson) or a waterbag density profile (Strasburg and Davidson).

Theoretical Model

- Define

$$s \equiv \beta_b c t \qquad \kappa_f \equiv \omega_{\beta b}^2 / \beta_b^2 c^2$$

$$\psi(r,s) = \frac{q_b}{\gamma_b^3 m_b \beta_b^2 c^2} \phi(r,s).$$

- Radial orbit equation for a test particle is

$$\frac{d^2 r}{ds^2} + \left(\kappa_f + \frac{1}{r}\frac{\partial \psi^0}{\partial r} + \frac{1}{r}\frac{\partial \delta\psi}{\partial r} \right) r = \frac{\bar{P}_\theta^2}{r^3},$$

- For a matched beam, and $\delta\psi = 0$, the test particle motion is regular.
- For a matched beam, and $\delta\psi \neq 0$, the nonlinear oscillatory force $(-\partial\delta\psi/\partial r)$ can induce chaotic particle motion, and eject particles from the beam core.

Poincare Plot: Low Beam Intensity

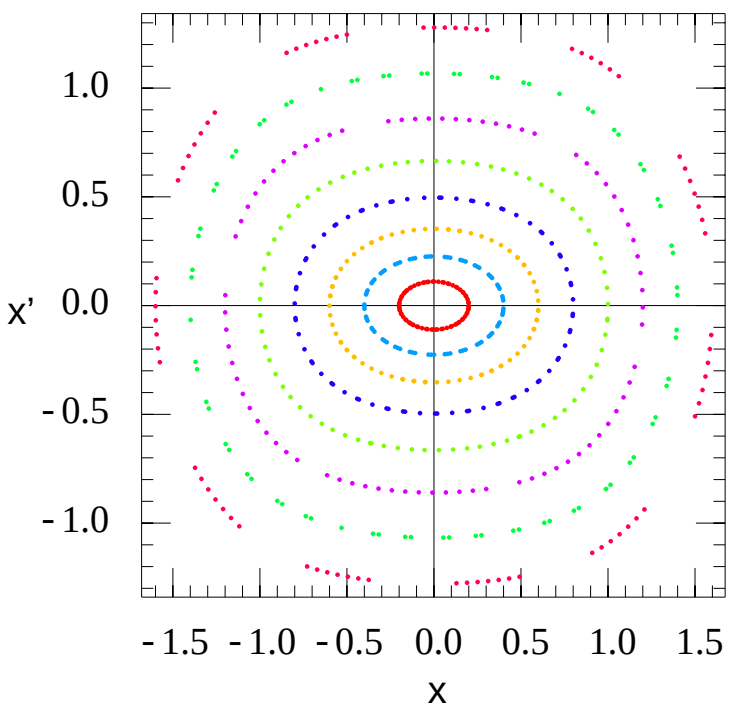

(a) $\frac{\nu}{\nu_0} = 0.54$, $s_b = 0.7$, $\frac{\delta n_b}{n_b} = 0$

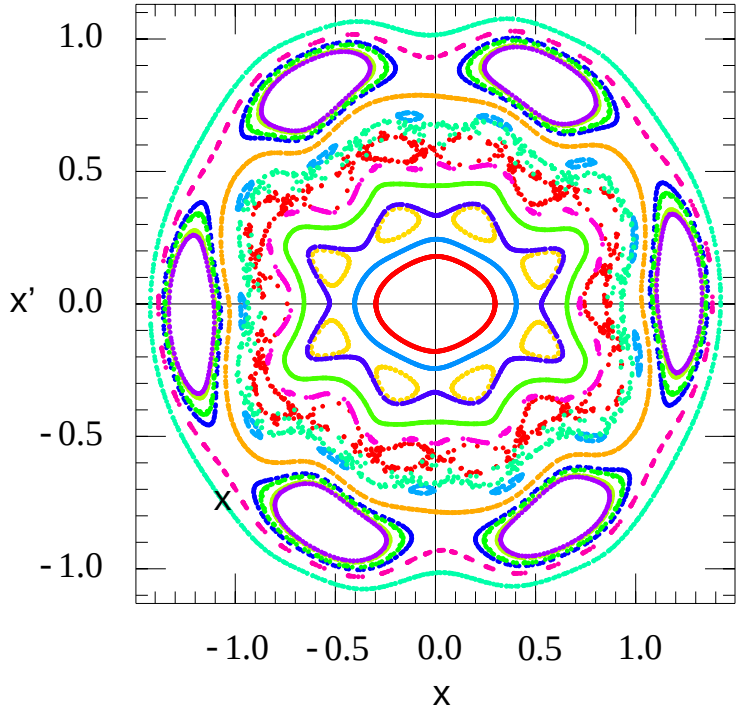

(b) $\frac{\nu}{\nu_0} = 0.54$, $s_b = 0.7$, $\frac{\delta n_b}{n_b} = 10\%$

Poincare Plot: High Beam Intensity

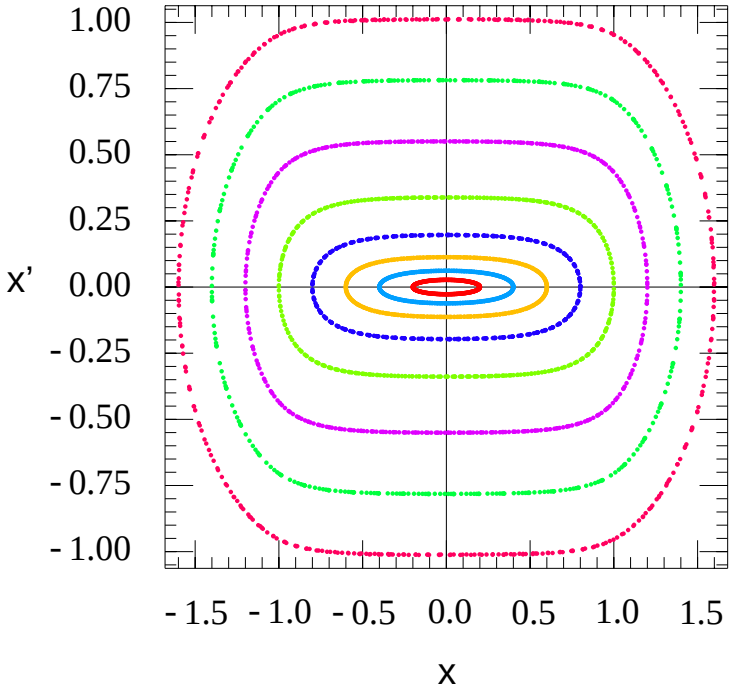

(a) $\frac{\nu}{\nu_0} = 0.13, s_b = 0.98, \frac{\delta n_b}{n_b} = 0$

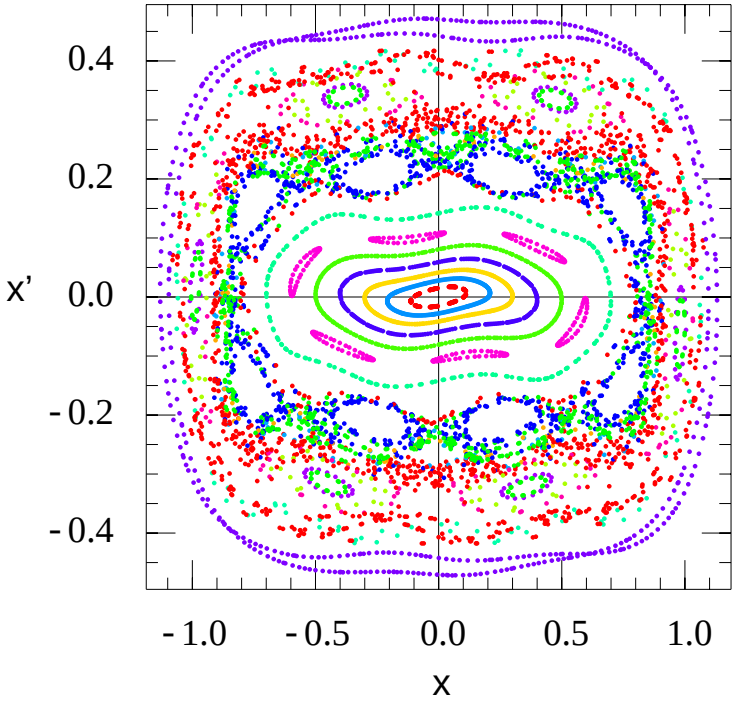

(b) $\frac{\nu}{\nu_0} = 0.13, s_b = 0.98, \frac{\delta n_b}{n_b} = 1.0\%$

Poincare Plot: High Beam Intensity, Moderate Mode Amplitude

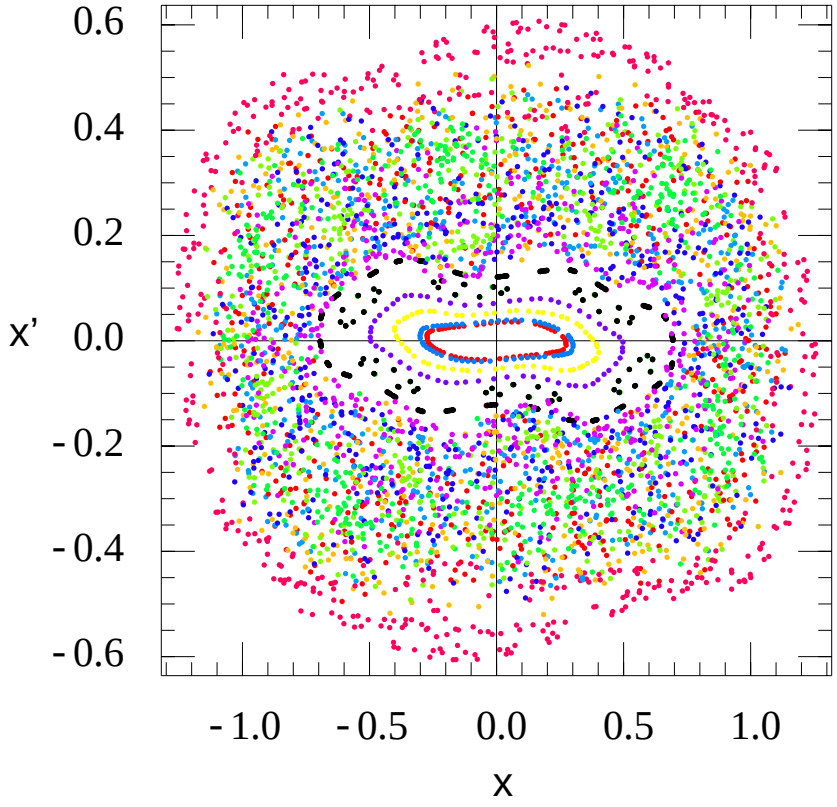

System Parameters:

$$\frac{\nu}{\nu_0} = 0.13, \qquad s_b = 0.98, \qquad \frac{\delta n_b}{n_b} = 2.5\%$$

Location of Resonances in Phase Space

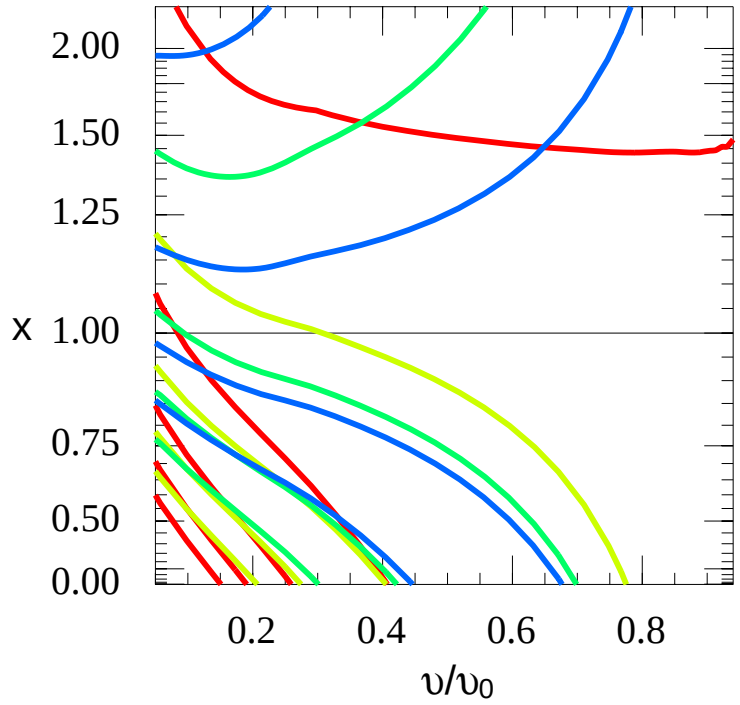

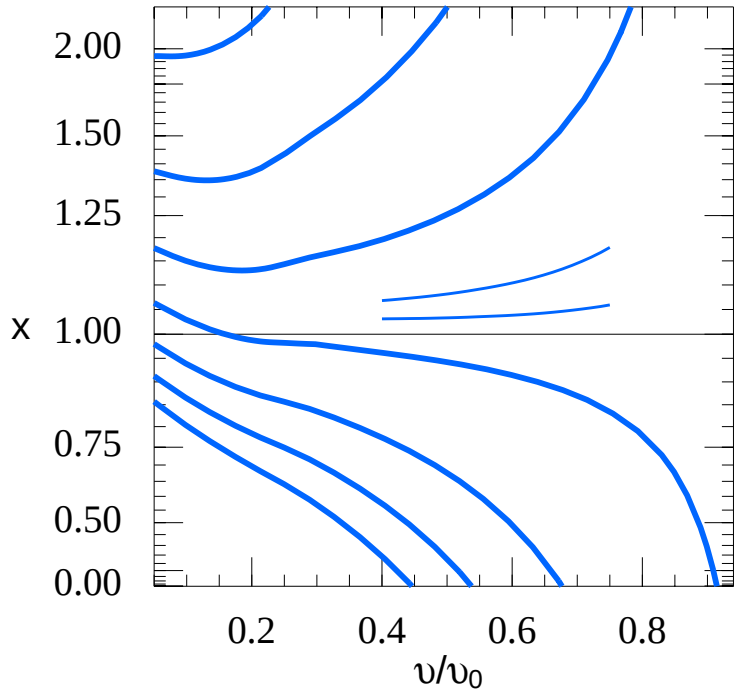

$n = 1, \quad 2, \quad 3, \quad 4$

For $\nu/\nu_0 = 0.54$ with large amplitude perturbations, island chains are visible ($\star$) for 6:1, 13:2, 20:3, 7:1, and 8:1 resonances, and their locations are very accurately predicted by analytic theory.

Presentation Outline

- Nonlinear stability theorem
- Nonlinear perturbative simulations (BEST code)
- Collective two-stream interactions
- Instability driven by temperature anisotropy ($T_{\perp b} \gg T_{\|b}$).
- Hamiltonian averaging techniques
- Halo particle production by collective excitations
- ⇨ Paul Trap Simulator Experiment

Paul Trap Simulator Experiment

Objective:

- Simulate collective processes and transverse dynamics of intense charged particle beam propagation through an alternating-gradient quadrupole focusing field using a compact laboratory Paul trap.

Approach:

- Investigate dynamics and collective processes in a long one-component charge bunch confined in a Paul trap with oscillating wall voltage $V_0(t+T) = V_0(t)$.

References:

- "A Paul Trap Configuration to Simulate Intense Nonneutral Beam Propagation Over Large Distances Through a Periodic Focusing Quadrupole Magnetic Field," R. C. Davidson, H. Qin, and G. Shvets, Physics of Plasmas **7**, 1020 (2000).
- "Paul Trap Experiment for Simulating Intense Beam Propagation Through a Quadrupole Focusing Field," R. C. Davidson, P. Efthimion, R. Majeski, and H. Qin, Proceedings of the 2001 Particle Accelerator Conference, 2978 (2001).
- "Paul Trap Simulator Experiment to Simulate Intense Beam Propagation Through a Periodic Focusing Quadrupole Field," R. C. Davidson, P. C. Efthimion, E. Gilson, R. Majeski, and H. Qin, American Institute of Physics Conference Proceedings **606**, 576 (2002).

Paul Trap Simulator Configuration

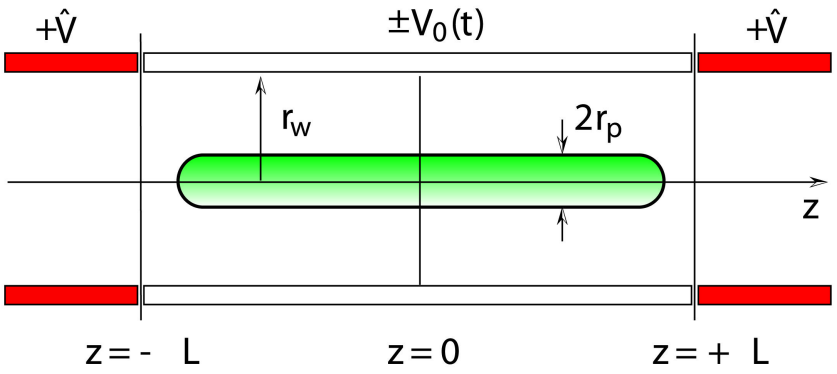

(a)

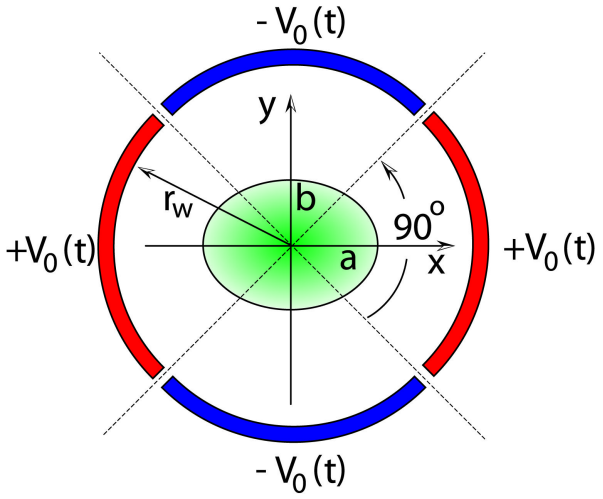

(b)

Paul Trap Simulator Experiment

Nominal Operating Parameters

Plasma column length	2 m
Wall electrode radius	10 cm
Plasma column radius	1 cm
Maximum wall voltage	400 V
End electrode voltage	400 V
Voltage oscillation frequency	100 kHz

Transverse Hamiltonian for Intense Beam Propagation

Transverse Hamiltonian (dimensionless units) for intense beam propagation through a periodic focusing quadrupole magnetic field is given by

$$H_{\perp}(x, y, x', y', s) = \frac{1}{2}(x'^2 + y'^2) + \frac{1}{2}k_q(s)(x^2 - y^2) + y\,(x, y, s)$$

where $x' = dx/ds,\ y' = dy/ds,\ y\,(x, y, s) = e_b f^{s}(x, y, s)/g_b^3 m_b b_b^2 c^2$

and

$$k_q(s) = \frac{e_b B_q'(s)}{g_b m_b b_b c^2}$$

with

$$k_q(s + S) = k_q(s)$$

Transverse Hamiltonian for Particle Motion in a Paul Trap

Transverse Hamiltonian (dimensionless units) for a long charge bunch in a Paul trap with time periodic wall voltages $V_0(t+T)=V_0(t)$ is given by

$$H_\perp(x,y,\dot{x},\dot{y},s)=\frac{1}{2}(\dot{x}^2+\dot{y}^2)+e_b f_{ap}(x,y,t)+e_b f^s(x,y,t)$$

where the applied potential $(0\le r\le r_w)$

$$f_{ap}(x,y,t)=\frac{4V_0(t)}{p}\sum_{\ell=1}^{\infty}\frac{\sin(\ell p/2)}{\ell}\left(\frac{r}{r_w}\right)^{2\ell}\cos(2\ell q)$$

can be approximated by (for $r_p << r_w$)

$$f_{ap}(x,y,t)=\frac{1}{2}k_q(t)(x^2-y^2),\ \text{where}\ k_q(t)=\frac{8e_bV_0(t)}{m_b p\ r_w^2}$$

Paul Trap Simulator Experiment

Planned experimental studies include:

- Beam mismatch and envelope instabilities.
- Collective wave excitations.
- Chaotic particle dynamics and production of halo particles.
- Mechanisms for emittance growth.
- Effects of distribution function on stability properties.

Plasma is formed using a cesium source or a barium coated platinum or rhenium filament. Plasma microstate will be determined using laser-induced fluorescence (Levinton, FP&T).

Paul Trap Simulator Experiment

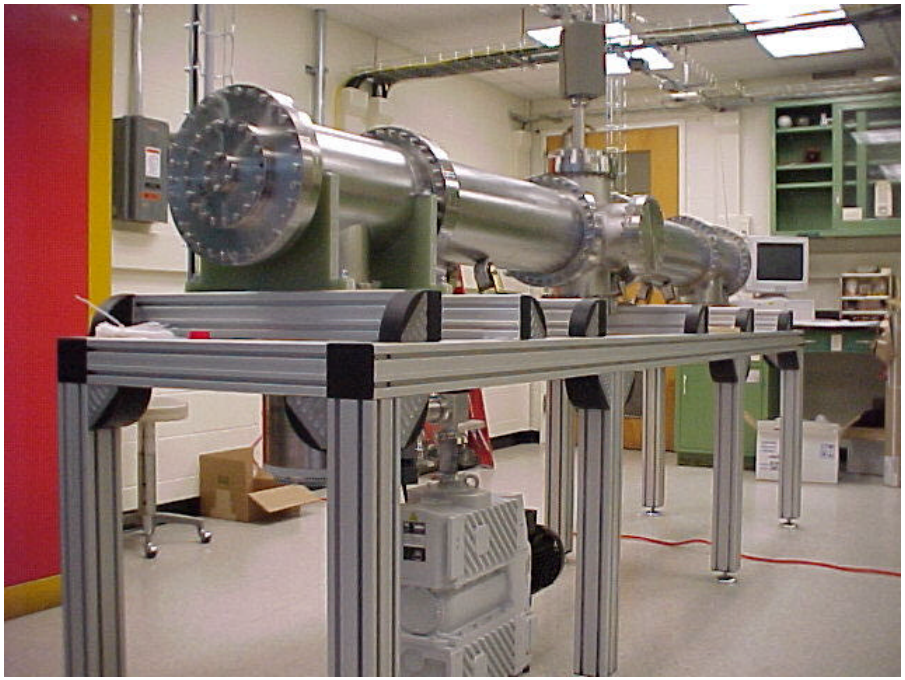

Paul Trap Simulator Experiment vacuum chamber.

- Laboratory preparation, procurement, assembly, bakeout, and pumpdown of PTSX vacuum chamber to 5.25×10^{-10} Torr (May, 2002).

Paul Trap Simulator Experiment

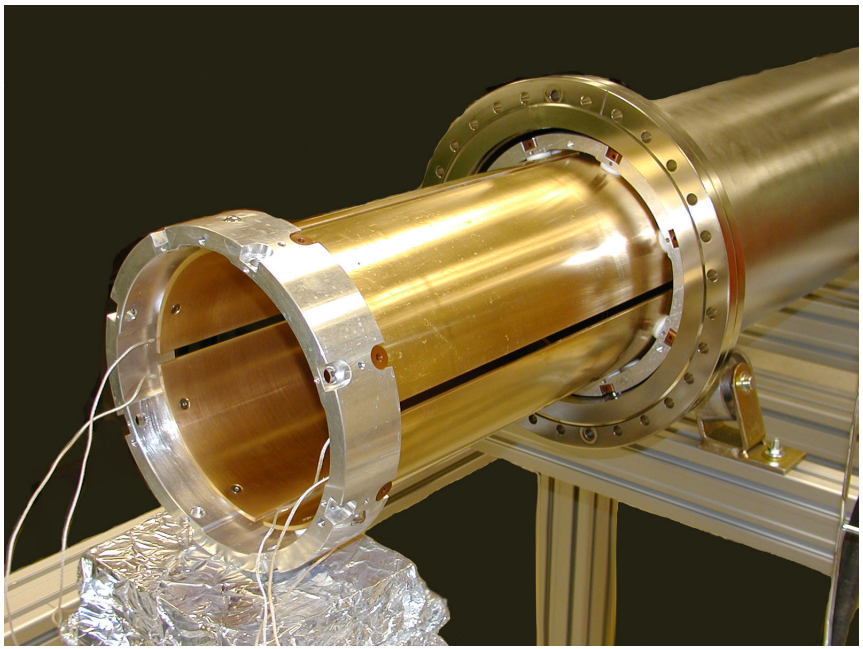

Paul Trap Simulator Experiment electrodes.

- Stainless steel gold-plated electrodes are supported by aluminum rings, teflon, and vespel spacers.

Paul Trap Simulator Experiment

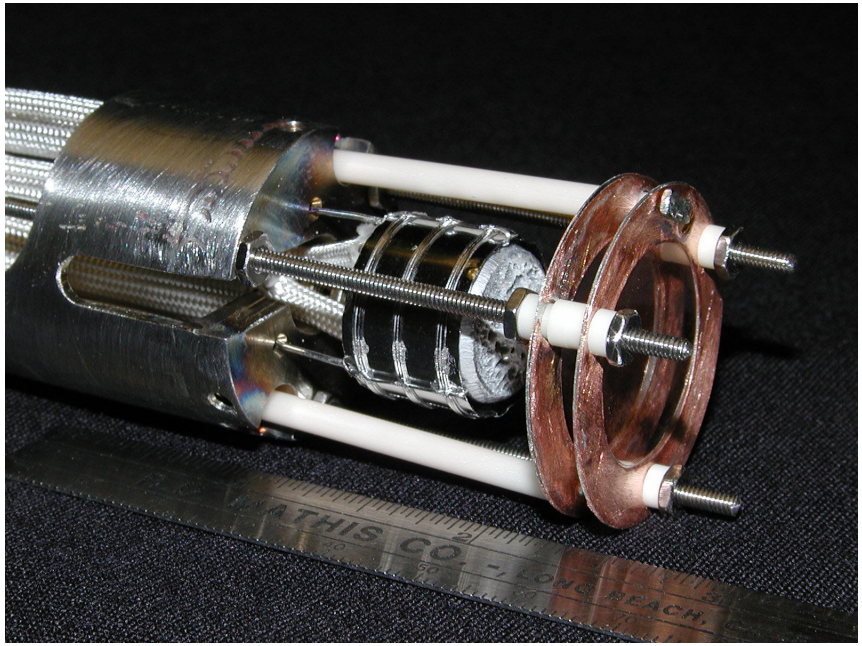

Paul Trap Simulator Experiment cesium source.

- Aluminosilicate cesium source produces up to 30 μA of ion current when a 200 V acceleration voltage is used.

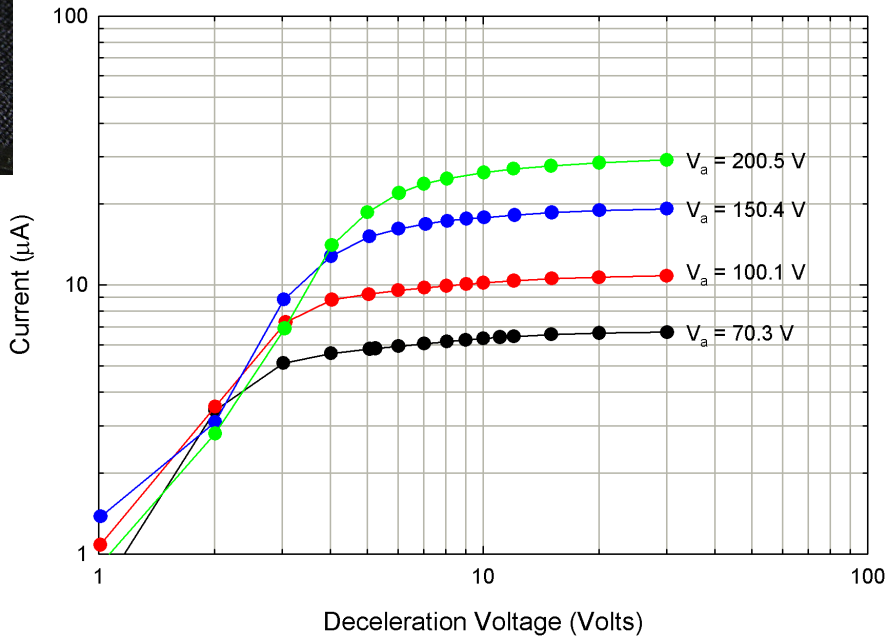

Paul Trap Simulator Experiment

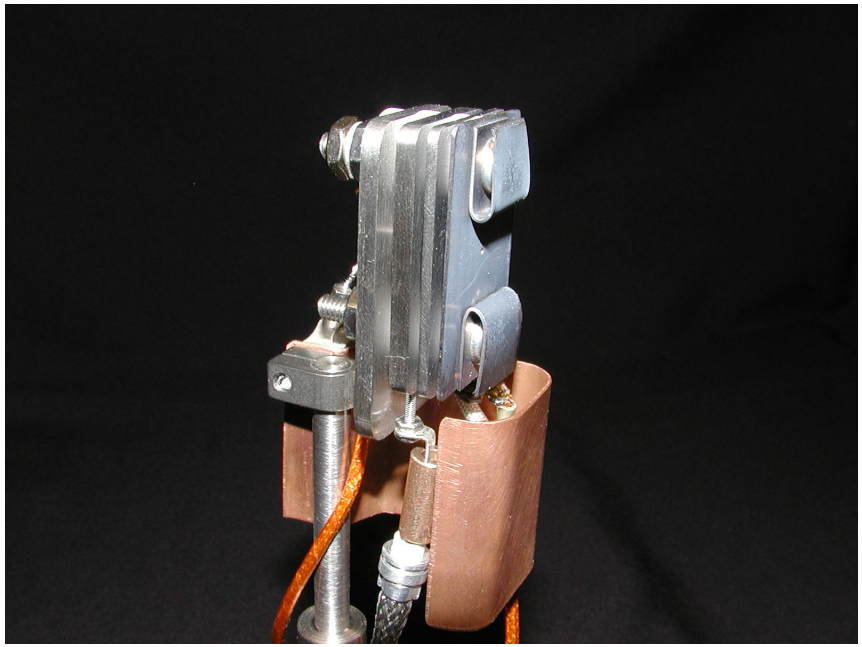

Paul Trap Simulator Experiment Faraday cup.

- Faraday cup with sensitive electrometer allows 20 fC resolution. Linear motion feedthrough with 6" stroke allows measurement of radial density dependence.

Paul Trap Simulator Experiment

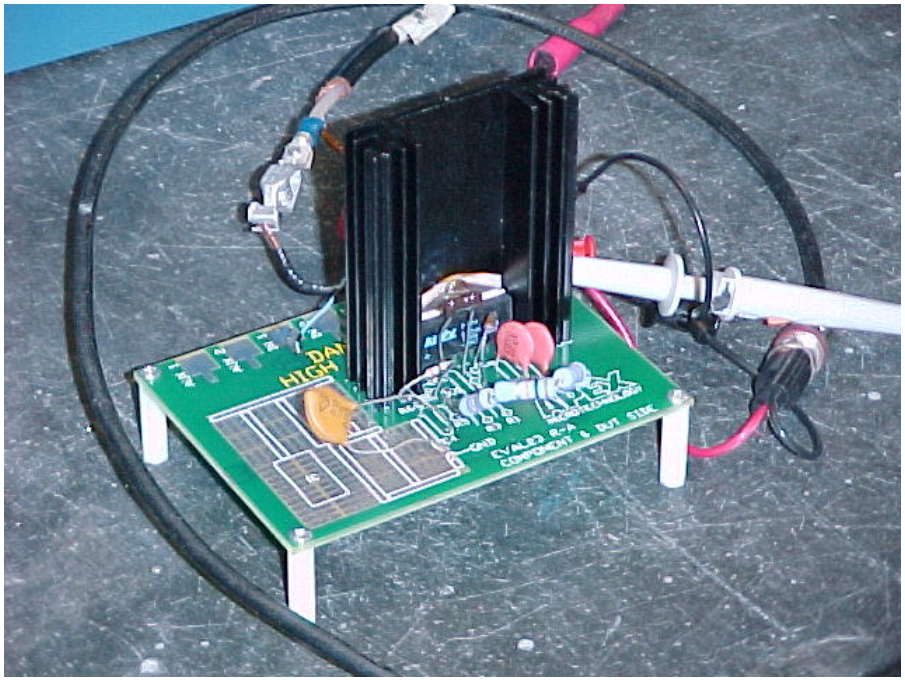

Paul Trap Simulator Experiment electrode driver test circuit.

•Electrode driver development using high voltage power op-amp to apply 400 V, 100 kHz signals to electrodes (February, 2002).

Paul Trap Simulator Experiment Initial Results

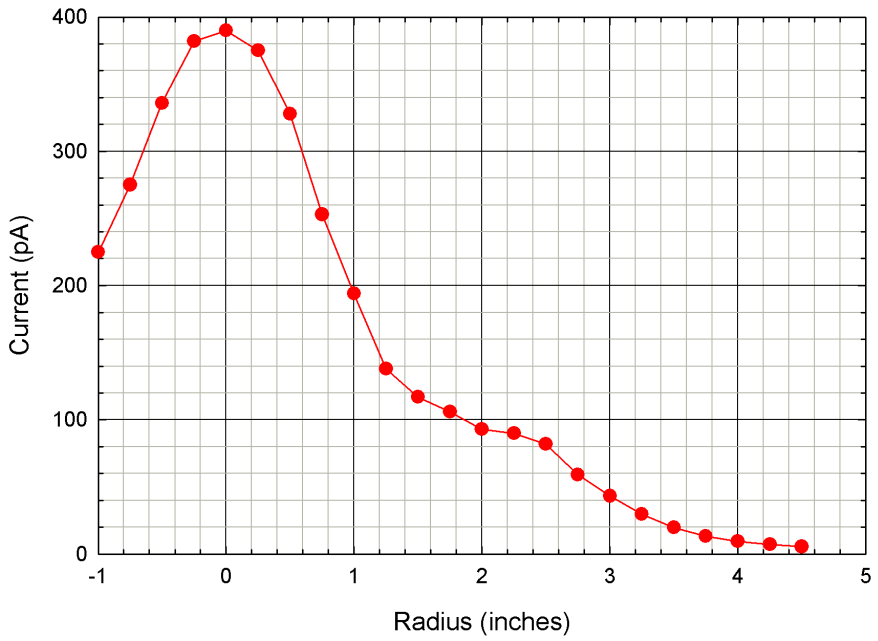

Current collected on Faraday cup versus radius.

- Experiment - stream Cs^+ ions from source to collector without axial trapping of the plasma.

Electrode parameters:

- $V_0(t) = V_{0\,max} \sin(2p\,f\,t)$
- $V_{0\,max} = 387.5$ V
- $f = 90$ kHz

Ion source parameters:

- $V_{accel} = -183.3$ V
- $V_{decel} = -5.0$ V

Conclusions

- Considerable progress has been made in developing and applying advanced theoretical techniques and simulation capabilities based on the nonlinear Vlasov-Maxwell equations to describe intense beam propagation.

- Quite remarkably, these capabilities can be applied over the entire range of normalized beam intensity

$$0 < \frac{\hat{\omega}_{pb}^2}{2\gamma_b^2 \omega_{\beta\perp}^2} < 1\,.$$

- Advanced simulation studies benefit considerably from comparisons with analytical results and experiment.

- Stay tuned for experimental results from the Paul Trap Simulator Experiment (PTSX).